Am J Cancer Res 2012;2(1):93-103
www.ajcr.us /ISSN:2156-6976/ajcr0000091

Original Article

Molecular signature and pathway analysis of human primary squamous and adenocarcinoma lung cancers

Nikolai Daraselia[1], Yipeng Wang[2], Adam Budoff[2], Alexander Lituev[3], Olga Potapova[3], Gordon Vansant[2], Joseph Monforte[2], Ilya Mazo[1], and Valeria S Ossovskaya[4]

[1]Ariadne Inc., Rockville, MD, USA; [2]AltheaDx, San Diego, CA, USA; [3]Cureline Inc., South San Francisco, CA, USA; [4]BiPar Sciences, Inc. (subsidiary of Sanofi), South San Francisco, CA, USA

Received September 29, 2011; accepted October 22, 2011; Epub November 19, 2011; Published January 1, 2012

Abstract: Non-small cell lung cancer (NSCLC) is the most common type of lung cancer, with a poor response to chemotherapy and low survival rate. This unfavorable treatment response is likely to derive from both late diagnosis and from complex, incompletely understood biology, and heterogeneity among NSCLC subtypes. To define the relative contributions of major cellular pathways to the biogenesis of NSCLC and highlight major differences between NSCLC subtypes, we studied the molecular signatures of lung adenocarcinoma (ADC) and squamous cell carcinoma (SCC), based on analysis of gene expression and comparison of tumor samples with normal lung tissue. Our results suggest the existence of specific molecular networks and subtype-specific differences between lung ADC and SCC subtypes, mostly found in cell cycle, DNA repair, and metabolic pathways. However, we also observed similarities across major gene interaction networks and pathways in ADC and SCC. These data provide a new insight into the biology of ADC and SCC and can be used to explore novel therapeutic interventions in lung cancer chemoprevention and treatment.

Keywords: NSCLC, adenocarcinoma, squamous cell carcinoma, molecular signature, gene expression, pathway

Introduction

Worldwide, over 1.3 million people are diagnosed each year with lung cancer, with over 1.1 million deaths [1, 2]. Lung cancer is the most common global cause of cancer death in men and second only to breast cancer in women (17.6% of cancer-related deaths in both sexes) [1-3]. There is a high fatality rate with this disease, with only 15% of patients still alive 5 years after diagnosis [4]. Non-small cell lung cancer (NSCLC) is the most common type of lung cancer, accounting for 85% of cases, and can be divided into three main subgroups: adenocarcinoma (ADC; 30-50% of cases), squamous cell carcinoma (SCC; ~30%), and large cell carcinoma (LCC; ~10%), according to the predominant morphology of the tumor cells as determined by light microscopy [4-7]. NSCLC is associated with high rates of proliferation and metastases, as well as poor prognosis for advanced-stage disease compared with other cancers. There are several potential explanations for the disparity between lung cancer survival and other common tumors, including late detection and histologic heterogeneity. This heterogeneity is reflected by the fact that the majority of prostate, breast, and colorectal carcinomas are ADC, while only 30% of NSCLC cases are of this subtype [6, 8]. For the most part, and until recently, NSCLC subtypes (SCC, LCC, and ADC) were treated similarly, regardless of the biologic heterogeneity associated with histology. It is likely that poor historic lung cancer response rates may be attributable in part to a relatively homogenous approach to treat a heterogeneous disease. Therefore, a better understanding and molecular characterization of the NSCLC subtypes could contribute to improved design of treatment schedules and management of lung cancer.

Gene expression profiling using microarrays is a robust and straightforward way to study the molecular features of different types and subtypes of cancer at a systems level. Although it is possible to distinguish the different NSCLC subgroups histologically, genomic profiling demonstrates that there are significant and distinct differences in the molecular signature associ-

ated with each subtype. The objective of this study was to enhance the understanding of NSCLC pathogenesis through characterization of molecular and pathway signatures in primary lung ADC and SCC samples, and to compare these signatures with those of normal lung tissue.

Materials and methods

Isolation of RNA

Sets of syngeneic normal and tumor samples (lung ADC and SCC) were obtained from Cureline Biobank (Cureline Inc., San Francisco, CA). Eighty formalin-fixed, paraffin-embedded (FFPE) tissue samples from 20 patients with NSCLC were analyzed (20 FFPE tissue samples for each group). For RNA isolation, five 10-μm sections were sliced via microtome, placed in 1.7 ml tubes, and deparaffinized with 1 ml of xylene (EMD Chemicals, Gibbstown, NJ). The samples were digested for 16 hours with Proteinase K and total RNA isolation was performed using the Epicentre Biotechnologies MasterPure™ Complete DNA and RNA Purification Kit (Epicentre Biotechnologies, Madison, WI) following the manufacturer's instructions. All samples were subsequently treated with RNase-free DNase I (Ambion, Austin, TX).

Synthesis of cDNA, amplification, and labeling

RNA samples were amplified and converted to cDNA using the NuGEN WT-Ovation FFPE v2 RNA Amplification System (NuGEN Technologies, San Carlos, CA) [9, 10]. Briefly, 50 ng of RNA was reverse transcribed to antisense-cDNA, amplified using kit reagents, and purified using a QIAGEN PCR purification kit (QIAGEN, Valencia, CA). DNA concentration was assessed using a Nanodrop ND-100 spectrophotometer. Sense transcript cDNA (ST-cDNA) was generated from 2-4 μg of purified antisense-cDNA using the kit reagents according to manufacturer's instructions. ST-cDNA was purified by QIAGEN kit and final DNA concentration determined by absorption. Up to 5 μg of purified ST-cDNA was fragmented and biotin-labeled using the NuGEN Encore Biotin Module Kit (NuGEN Technologies, San Carlos, CA).

Hybridization, washing, and analysis

Biotin-labeled cDNA from each sample was directly hybridized to GeneChip Human Gene 1.0 ST Arrays (Affymetrix, Santa Clara, CA) along with GeneChip Eukaryotic Hybridization controls (Affymetrix, Santa Clara, CA). Samples were incubated at 45°C in an Affymetrix hybridization oven 640 at 60 rpm for 16 hours, and washed with an Affymetrix GeneChip Fluidics Station 450 according to the manufacturer's specifications. Scanning was performed using the Affymetrix GeneChip 7G scanner using manufacturer-recommended default settings.

Data analysis

An Affymetrix Expression Console was used to generate quality control parameters, process probe intensity files and CEL-format data files, and to normalize and summarize a gene expression measurement for each probe set on the array through a Robust Multiarray Averaging (RMA) algorithm [11]. All the clinical and control samples in the study and the expression values were log-transformed with a base of 2 for downstream data analysis. For each individual sample, differential expression profiles of cancer versus normal syngeneic tissue were calculated. In addition, differential profiles of all cancer samples versus all normal breast samples were calculated using an unpaired t-test.

All gene expression analyses were performed in Pathway Studio 7 (Ariadne Genomics, Inc., Rockville, MD) [9, 11-15], using the ResNet 7 database (Ariadne Genomics, Inc.) [9, 10]. Enrichment analysis in Pathway Studio 7 was performed by Gene Set Enrichment Analysis (GSEA) [16] and Sub-Network Enrichment Analysis (SNEA) algorithms (Supplementary Figure 1S) [11]. Functional enrichment was performed using Fisher's Exact Test.

SNEA enrichment in Pathway Studio was calculated using the Mann-Whitney test, a non-parametric method that compares the medians of non-normal distributions X and Y. Both samples (having sizes *N* and *M*) are combined into one array in ascending order with each element then replaced by its rank in the array from 1 to N+M. The ranks of the first sample elements are summarized and a Mann-Whitney U-value calculated from **Equation 1**:

$$U = NM + \frac{N(N+1)}{2} - \sum_{x_i} Rank(x_i) \qquad \textbf{Eq. 1}$$

If U is close to the mean of U (i.e. 0.5·N·M) then the medians of X and Y are similar. The significance level of the U statistic can be derived from the distribution quantiles. When applied to gene expression data, two distributions are typically derived from the gene set or sub-network, and from the entire gene expression profile measured on the chip. The following steps describe the computational steps performed by the SNEA algorithm.

Preparation of sub-networks

SNEA was used to build sub-networks from the relationships in a database based on criteria specified by the user. A central 'seed' is initially created from all relevant entities in the database, and associated entities retrieved based on their relationship with the seed (binding partners, expression targets, protein modification targets, etc.).

Calculation of background distribution

This algorithm was used to calculate a background distribution of all expression values for the selected sample in the experiment, typically from a differential measurement such as that resulting from the 'Find Differentially Expressed Genes' tool.

Calculation of sub-network distribution

This algorithm was used to create a 'sub-network' distribution of the expression values in a similar manner for all sub-networks constructed in the previous step. More importantly, during distribution calculation, the expression value for each entity connected to a seed is accounted for as many times as the connectivity of that entity in ResNet. The purpose of this correction is to correct the bias introduced by the different connectivity of entities in ResNet.

Statistical comparison of sub-network distribution with background distribution

This algorithm is used to compare the sub-network distribution with the background distribution using a one-sided Mann-Whitney U-test, and calculates a p-value indicating the statistical significance of difference between two distributions. Presentation and prioritization of results were done with Pathway Studio, which presents the 'seed' entity for each sub-network along with the sub-networks themselves in the user interface, ranked from the lowest (best) to the highest (worst) p-value. Note: the percentage overlap is also presented in order to provide an adequate measurement of significance and confidence in various statistical tests of overlap.

Analysis of key regulators of differential gene expression

The key regulators of differential response are those components of signal transduction pathways and expression regulators that are most likely to be involved in the regulation of genes differentially expressed between tumor and normal samples. Such key regulatory signaling pathways are assumed to be deregulated (e.g. abnormally activated or suppressed) in a disease state and provide insights into the mechanisms and molecular features of a disease. Our analysis implements a proprietary SNEA algorithm, which utilizes a gene expression regulatory network built from facts extracted from the literature. The network is used to generate a comprehensive collection of gene sets, each representing immediate downstream neighbors of each individual protein in the network. It is assumed that if the downstream expression targets of the central seed protein are enriched with differentially expressed genes (i.e. the sub-network is found to be statistically significant in enrichment analysis), then the seed protein is one of the key regulators of the observed differential response. As sub-networks are constructed from all the proteins in the entire expression network, including ligands, receptors, signaling proteins, and transcription factors, the seed proteins of statistically significant sub-networks presumably constitute the components of a regulatory network involved in the modulation of the observed differential response.

Results

Significant regulators of ADC and SCC

We focused our analysis on the regulation of major cellular pathways. The key regulators of differential response were identified by searching for all expression sub-networks in the ResNet 7 database enriched with differentially changed genes using a Mann-Whitney test with a p-value cut-off of 0.001. We performed analyses separately for lung SCC and ADC, and all

Table 1. Significant regulators in lung adenocarcinoma (ADC) and squamous cell carcinoma (SCC) by SNEA (Mann-Whitney p<0.001)

Name	Sub-network size	Median fold change	p-value
Adenocarcinoma			
CTGF	47	1.02072	8.98×10^{-5}
S100A4	15	1.28985	1.52×10^{-4}
Vitronectin receptor	21	1.14296	2.38×10^{-4}
E2F3	34	1.20872	3.45×10^{-4}
PDGF	285	1.01231	4.48×10^{-4}
miR-200	5	-1.52286	4.74×10^{-4}
E2F4	40	1.18259	8.11×10^{-4}
EMP2	5	-1.48652	8.50×10^{-4}
RB1	75	1.10424	8.61×10^{-4}
Squamous cell carcinoma			
PDGF	285	-1.03133	$3.05 \text{ X } 10^{-5}$
EGF	393	-1.01802	$3.33 \text{ X } 10^{-5}$
CTGF	47	-1.03683	2.61×10^{-4}
CX3CL1	11	-1.45216	4.38×10^{-4}
E2F4	40	1.3792	4.98×10^{-4}
IL1F8	34	-1.11308	5.47×10^{-4}
E2F3	34	1.3792	8.09×10^{-4}
PRKCB	33	-1.17599	8.97×10^{-4}
COMP	9	-1.45216	9.25×10^{-4}

identified significant regulators are shown in **Table 1.** We found that transcription factors associated with differential expression in both ADC and SCC, in comparison with normal lung tissue, were representatives of the E2F family (E2F3 and E2F4). The connective tissue growth factor (CTGF) and platelet-derived growth factor (PDGF) pathways are also significantly changed in both subtypes of NSCLC. The retinoblastoma (Rb1) pathway is up-regulated specifically in ADC, whereas the epidermal growth factor (EGF) pathway is significantly affected (down-regulated) only in SCC. Lung ADC samples show significant and specific down-regulation of the miR-200 molecular network and the epithelial membrane protein 2 (EMP2). The miR-200 family of microRNAs plays a major role in specifying the epithelial phenotype by preventing expression of the transcription repressors ZEB1/deltaEF1 and SIP1/ZEB2, and regulates epithelial-mesenchymal transition [17]. EMP2 controls surface levels of several classes of integrin and other cell-interaction molecules, and their trafficking to glycolipid-enriched lipid raft domains is important in receptor signaling [18]. Lung SCC samples show down-regulation of chemokine (C-X3-C motif) ligand 1 (CX3CL1), interleukin-1 family member 8 (IL1F8), and protein kinase C beta (PRKCB) pathways.

DNA repair, cell proliferation, and apoptotic pathways

DNA damage repair is a complex and multifaceted process that is critical to cancer cell survival and response to DNA-damaging chemotherapy. To define the relative contributions of DNA repair to ADC and SCC, we investigated the differential changes in all known DNA repair pathways. The record of genes and proteins involved in the regulation of DNA repair pathways were assembled using the ResNet 7 database and then verified as described previously [19]. **Figures 1, 2,** and **3** show graphically the changes in differential gene expression between all lung cancer samples and normal tissue among DNA-repair pathways, cell-cycle pathways, and apoptosis pathways, respectively, and defined by differential changes of the pathway proteins. Individual gene expression differences and p-values for components of each of these pathway types are provided in Supplementary **Tables S1, S2,** and **S3**, respectively.

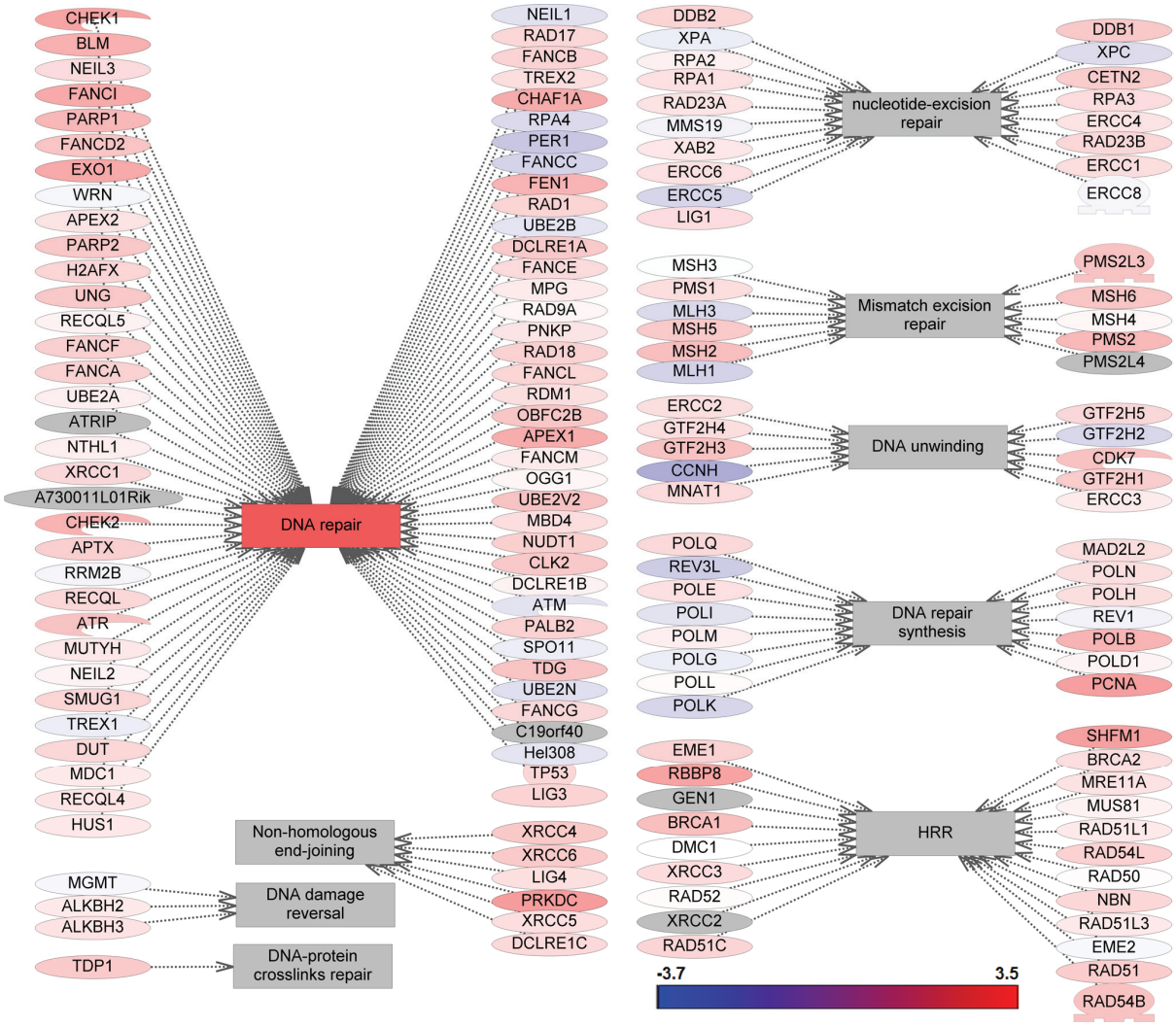

Figure 1. Gene expression changes in DNA repair pathways.

DNA repair components significantly up-regulated (2-fold or more with $p<0.001$) in lung SCC included retinoblastoma-binding protein 8 (RBBP8), protein kinase DNA-activated catalytic polypeptide (PRKDC), split hand/foot malformation (ectrodactyly) Type 1 (SHFM1), and proliferating cell nuclear antigen (PCNA). By contrast, there were no significant changes in expression of DNA-repair genes in lung ADC.

Cell-cycle genes were more significantly up-regulated in SCC than in ADC. Topoisomerase (DNA) II alpha (170 kD) (TOP2A), cyclin B1 (CCNB1), maternal embryonic leucine-zipper kinase (MELK), mitotic arrest deficient-like 2 (yeast), human homolog like-1 (MAD2L1), stratifin (SFN), cell division cycle 6 homolog (CDC6), abnormal spindle-like microcephaly-associated protein (ASPM), and DNA topoisomerase binding protein 1 (TOPBP1) were all significantly up-regulated in SCC. By contrast, only TOP2A was significantly up-regulated in ADC.

Among apoptotic pathways, CASP8 and FADD-like apoptosis regulator (CFLAR) was significantly down-regulated (-2.34) in SCC. No other apoptotic proteins were significantly changed in any of the ADC or SCC samples.

The SNEA approach was also applied to identify key regulators and detect global cell proliferation processes significantly affected in NSCLC.

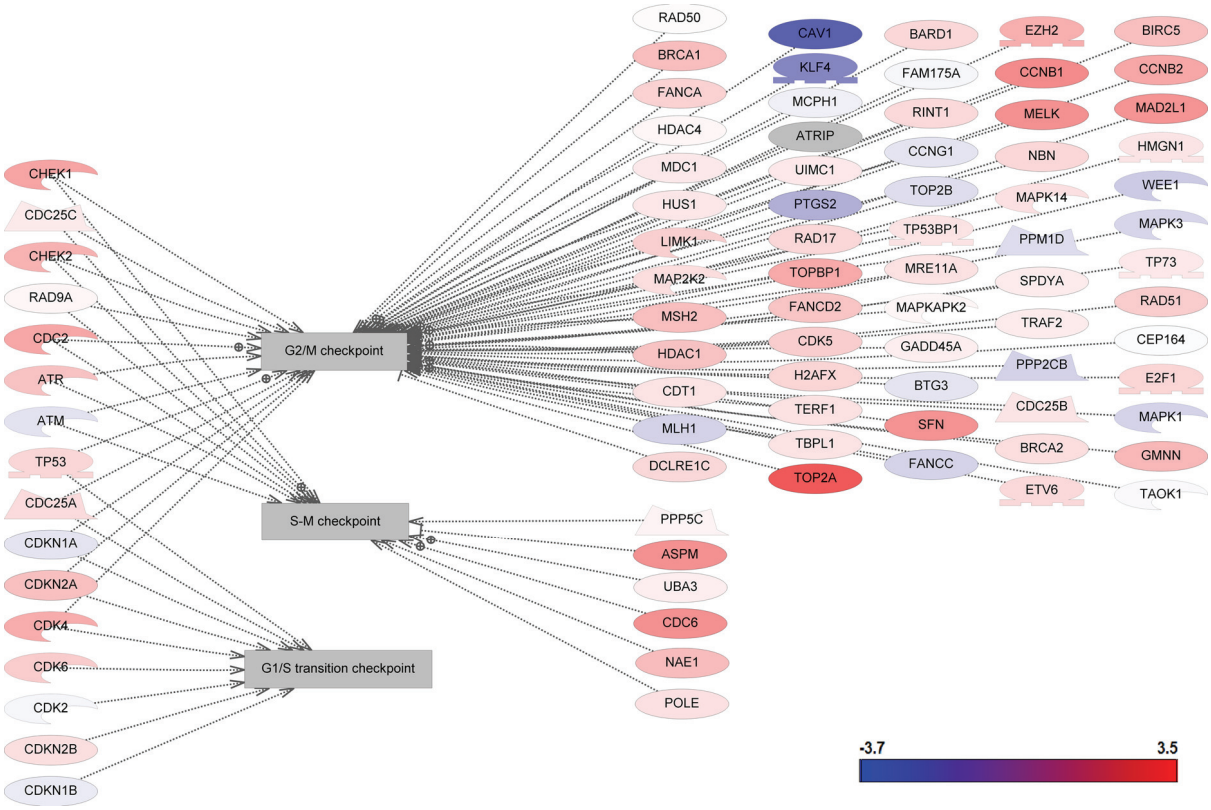

Figure 2. Gene expression changes in cell cycle pathways.

In this approach, sub-networks were built around each cell process in the ResNet 7 database and contained all proteins known to be involved in the regulation of the process (SNEA was applied with a Mann-Whitney p-value cut-off value of 0.001). Significantly affected processes are documented in **Table 2**. Most of the significantly affected processes in both lung cancer subtypes are related to cellular proliferation (spindle assembly, chromosome segregation, cytokinesis, kinetochore assembly, mitotic checkpoint, etc.), as would be expected in actively proliferating lung tumor cells. Other cellular processes are related to metastasis, including extracellular matrix remodeling, cell invasion, and cell-cell contact. In general, changes were similar across subtypes.

Metabolic pathways

Because the cell cycle is functionally linked to cellular metabolism and energy production, we next analyzed the differential gene expression of ADC and SCC versus pathologically normal lung tissue and all metabolic pathways in the ResNet 7 database, using the GSEA algorithm, and a Mann-Whitney test with p-value cut-off at 0.05. Significantly changed metabolic processes for each lung cancer subtype are documented in **Table 3**. Purine and pyrimidine synthesis pathways were significantly up-regulated in both subtypes. The SCC type also demonstrated up-regulated energy production pathways for oxidative phosphorylation, glucose metabolism, and the tricarboxylic acid cycle. These findings are consistent with active DNA synthesis and active proliferation of lung cancer cells.

Oncogenes and tumor suppressors

Because oncogenes and tumor suppressors play a significant role in the regulation of cell proliferation, we next investigated a major molecular network of 273 oncogenes and 92 tumor suppressors in ADC and SCC using the ResNet 7 database. The oncogenes with at least 2-fold change ($p<0.001$) are documented in **Table 4**. All oncogenes in ADC, and most in SCC, with the exception of ECT2 (elevated 3.6-fold) and DCUN1D1 (elevated 2.7-fold), were significantly

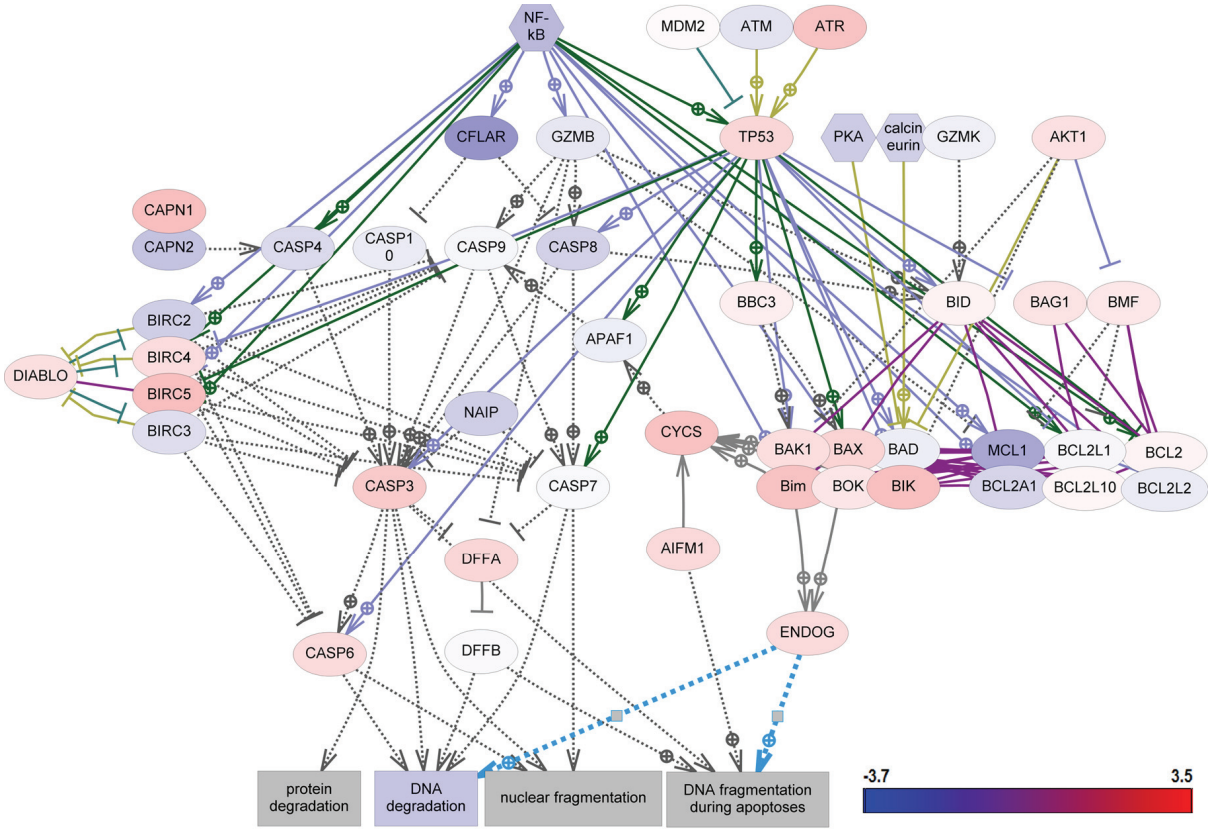

Figure 3. Gene expression changes in apoptotic pathways.

down-regulated. The oncogenes down-regulated in both types of lung cancer included FOS and FOSB. Changes in tumor suppressors were examined (**Table 4**) for both lung cancer subtypes. Tumor suppressors were not changed significantly in ADC, whereas in SCC, DLG1 and DLGAP5 were up-regulated, and TGFBR2 was down-regulated. Full details of differential changes in oncogenes and tumor suppressors (including p-values) are provided in Supplementary **Tables S4** and **S5**, respectively.

Discussion

NSCLC represents a heterogeneous collection of cancer subtypes that arise as a consequence of altered gene expression and mutations acquired during cancerogenesis. Molecular signatures of NSCLC subtypes can underline mechanisms of this complex disease and more importantly can facilitate the development of novel targeted therapy for cancer patients. Here we reported major cellular pathways of human lung ADC and SCC and described similarities as well as unique differences between these two subtypes of lung cancer.

Sub-Network Enrichment Analysis (SNEA)

To build comprehensive molecular signatures of ADC and SCC, we used the SNEA algorithm, which is designed to investigate variations in gene set enrichment. Unlike previously reported approaches, such as GSEA, which uses a predefined collection of hand-curated gene sets [16], SNEA uses the global literature-extracted gene-gene expression regulation network to generate a comprehensive collection of gene sets [11]. The global expression network used for SNEA in this study is extracted and comprised over 160,000 independently reported relations [11]. The advantage of the SNEA application for this type of analysis is in the unbiased knowledge-driven nature of this approach. Sub-networks in SNEA are calculated from gene expression regulation 'facts' extracted across the entire PubMed database. Thus, each individual relation can come from specific and perhaps very nar-

Table 2. Cellular processes significantly changed in lung adenocarcinoma (ADC) and squamous cell carcinoma (SCC) by SNEA (Mann-Whitney p<0.001)

Cellular process	Sub-network size	Median fold change	p-value
Adenocarcinoma			
Wound healing	385	1.02072	2.19×10^{-6}
ECM proteins	571	1.0277	2.38×10^{-6}
Chromosome segregation	149	1.10384	7.32×10^{-6}
Tissue remodeling	168	1.05076	1.16×10^{-5}
Cell survival	1251	1.03351	6.44×10^{-5}
Cell invasion	486	1.02405	7.79×10^{-5}
Tissue invasion	40	1.11402	1.23×10^{-4}
Mitotic cell cycle	37	1.10189	2.31×10^{-4}
G2/M transition	465	1.05898	2.37×10^{-4}
Abscission	25	1.00683	2.82×10^{-4}
Oncogenesis	347	1.02691	4.62×10^{-4}
Mitotic entry	123	1.07766	4.95×10^{-4}
Centrosome separation	38	1.13508	5.83×10^{-4}
Drug resistance	244	1.04375	7.66×10^{-4}
Cell redox homeostasis	18	1.12308	7.79×10^{-4}
Cell motility	691	1.02671	7.94×10^{-4}
Mitotic checkpoint	57	1.11636	8.92×10^{-4}
Cell contact	929	1.02568	9.04×10^{-4}
Squamous cell carcinoma			
Chromosome segregation	149	1.1897	4.58×10^{-10}
Kinetochore assembly	126	1.23986	7.28×10^{-10}
Mitosis	924	1.05925	1.35×10^{-8}
Spindle assembly	386	1.08566	6.70×10^{-8}
Cytokinesis	291	1.05385	1.03×10^{-7}
ECM proteins	571	-1.02692	2.90×10^{-7}
Wound healing	385	-1.05074	2.44×10^{-6}
DNA replication initiation	41	1.3792	1.02×10^{-5}
Mitotic checkpoint	57	1.24069	1.03×10^{-5}
Cell invasion	486	-1.01081	1.20×10^{-5}
Mitotic spindle assembly	41	1.23754	2.72×10^{-5}
G2/M transition	465	1.05662	2.81×10^{-5}
Premeiotic DNA synthesis	17	1.44176	3.11×10^{-5}
Cell motility	691	-1.01698	3.41×10^{-5}
Mitotic entry	123	1.1247	3.64×10^{-5}
Drug resistance	244	1.01383	4.29×10^{-5}
DNA replication checkpoint	40	1.35065	5.73×10^{-5}
Genome instability	178	1.13299	7.80×10^{-5}
S phase	737	1.02773	2.19×10^{-4}
DNA unwinding	117	1.15665	2.39×10^{-4}
Tissue remodeling	168	-1.03451	3.11×10^{-4}
Chromosome condensation	174	1.05662	3.14×10^{-4}
Cell growth	2072	1.00691	3.18×10^{-4}
Centrosome separation	38	1.30654	4.21×10^{-4}
Translation	689	-1.01232	4.53×10^{-4}
Cell division	598	1.00883	4.69×10^{-4}
Chemosensitivity	129	1.03154	4.94×10^{-4}
Cell–cell contact	307	-1.04502	5.89×10^{-4}
rRNA processing	69	1.21023	6.52×10^{-4}

Table 3. Metabolic pathways significantly changed in lung adenocarcinoma (ADC) and squamous cell carcinoma (SCC) by GSEA (Mann-Whitney test, $p<0.05$)

Name	Sub-network size	Median fold change	p-value
Adenocarcinoma			
Nicotinate and nicotinamide metabolism	79	1.05861	2.953×10^{-3}
Glut/Gln/Pro metabolism	38	1.11358	1.0798×10^{-2}
Bile acids metabolism	41	1.04722	1.1389×10^{-2}
Pyrimidine metabolism	100	1.08111	1.784×10^{-2}
Purine metabolism	154	1.06749	1.8009×10^{-2}
Squamous cell carcinoma			
Respiratory chain and oxidative phosphorylation	74	1.16544	4.60×10^{-6}
Purine metabolism	154	1.03009	7.87×10^{-4}
Tricarboxylic acid cycle	27	1.13055	1.177×10^{-3}
Branched chain amino acids metabolism	55	1.06616	3.688×10^{-3}
Glucose metabolism	53	1.08078	7.449×10^{-3}
Aspartate metabolism	26	1.14841	8.051×10^{-3}
Folate biosynthesis	20	1.17777	1.2205×10^{-2}
Pyrimidine metabolism	100	1.09129	2.0488×10^{-2}
Mannose metabolism	33	1.0791	2.3137×10^{-2}
Amino sugars synthesis	19	1.13317	2.5646×10^{-2}

Table 4. Oncogenes and tumor suppressors significantly affected in lung adenocarcinoma (ADC) and squamous cell carcinoma (SCC)

Name	Description	Fold-change	p-value
Adenocarcinoma			
FOS	v-fos FBJ murine osteosarcoma viral oncogene homolog	-2.02	9.18×10^{-4}
FOSB	FBJ murine osteosarcoma viral oncogene homolog B	-2.14	4.87×10^{-4}
Squamous cell carcinoma			
ECT2	Epithelial cell transforming sequence 2 oncogene	3.59	2.55×10^{-8}
DCUN1D1	DCN1, defective in cullin neddylation 1, domain containing 1 (*S. cerevisiae*)	2.66	4.00×10^{-7}
JUN	jun oncogene	-2.30	7.39×10^{-9}
FOS	v-fos FBJ murine osteosarcoma viral oncogene homolog	-2.80	7.18×10^{-7}
ROS1	c-ros oncogene 1 , receptor tyrosine kinase	-2.97	8.79×10^{-9}
CXCL2	Chemokine (C-X-C motif) ligand 2	-3.65	2.45×10^{-8}
FOSB	FBJ murine osteosarcoma viral oncogene homolog B	-4.65	1.60×10^{-9}
DLG1	Discs, large homolog 1 (*Drosophila*)	2.41	3.46×10^{-5}
DLGAP5	Discs, large (*Drosophila*) homolog-associated protein 5	2.35	4.22×10^{-7}
TGFBR2	Transforming growth factor, beta receptor II (70/80 kDa)	-2.09	1.85×10^{-11}

row publications, but when combined together they provide an unbiased and comprehensive picture of cellular gene expression network. Another critically important power of SNEA is in its ability to find 'hidden' regulators, for example genes and proteins for which changes in cancer are not detected on the level of mRNA, but rather on a biologic activity level. This is particularly important for proteins for which activity is regulated at the post-transcriptional level, such as post-translational protein modification, protein stability, or degradation. The vast majority of cancer signaling pathways are activated or inactivated through phosphorylation of individual protein kinases, an event that is unlikely to be reflected on the level of mRNA measured in gene expression profiling. Similarly, activity of many transcription factors downstream of major signaling cascades is regulated by phosphorylation, and these changes will be overlooked in

traditional gene expression profiling. SNEA can detect such regulators by looking at the changes in downstream targets, rather than the gene/protein itself. Another important advantage of SNEA is its ability to summarize the individual gene expression changes and to project them to the system-level cellular signaling map.

Molecular complexity of ADC and SCC

Our search for key transcriptional regulators involved in differential changes using the ResNet 7 transcriptional network showed uniform involvement of E2F, CTGF, and PDGF in lung cancer pathogenesis. These observations are consistent with previous reports describing the role of CTGF and PDGF in lung cancer progression [20-22]. Our analysis showed that SCC can be uniquely characterized by the involvement of the EGF, IL1F8, and CX3CL1 pathways, while changes in Rb1, miR-200, and EMP2 targets are specific for ADC.

Consistent with the aggressively proliferative phenotype of lung cancer cells, the most significantly affected cellular processes were those involved in the cell cycle and metastasis. The biochemical 'signature' pinpoints changes in purine and pyrimidine biosynthesis and energy production pathways, and these changes were seen in both ADC and SCC. Up-regulation of cell-cycle-related genes was more profound in SCC than in ADC. DNA repair genes were also more profoundly up-regulated in SCC. There were no significant changes in apoptotic genes in either type of lung cancer. Surprisingly, we found that all oncogenes in ADC and most oncogenes in SCC were significantly down-regulated, including FOS and FOSB. In SCC, ECT2 and DCUN1D1 were up-regulated. Tumor suppressors were not changed significantly in ADC, whereas in SCC, the significantly changed tumor suppressors were DLG1 and DLGAP5 (elevated), and TGFBR2 (down-regulated).

In conclusion, we found that ADC and SCC subtypes of NSCLC can be characterized by unique gene signatures and distinct molecular pathways. Our data suggest that the gene expression signature of subtypes of lung cancer can be a critical tool for improved characterization of subtypes currently classified based on analysis of histology of tumor samples by light microscopy. Taken together, these data provide a better understanding of the unique molecular features of NSCLC subtypes, and may open new avenues towards the molecular-based identification of novel therapeutic strategies for NSCLC.

Acknowledgements

We thank Ann Contijoch, Sanofi, for reviewing this paper. Editorial assistance was provided by ArticulateScience Ltd., supported by Sanofi.

Conflict of interest

Valeria Ossovskaya is employee of BiPar Sciences Inc. (subsidiary of Sanofi). Yipeng Wang, Adam Budoff, Gordon Vansant, and Joseph Monforte are employees of AltheaDx Inc. Qiang Xu is former employee of AltheaDx Inc. Alexander Lituev and Olga Potapova are employees of Cureline Inc. Nikolai Daraselia is employee of Ariadne Inc.

Address correspondence to: Dr. Valeria S. Ossovskaya, BiPar Sciences, Inc. (subsidiary of Sanofi), 400 Oyster Point Blvd., Suite 200, South San Francisco, CA 94080 Tel: (650) 615-7019; Fax: (650) 615-7005; E-mail: valeria.ossovskaya@sanofi-aventis.com

References

[1] Ferlay J, Autier P, Boniol M, Heanue M, Colombet M and Boyle P. Estimates of the cancer incidence and mortality in Europe in 2006. Ann Oncol 2007; 18: 581-592.

[2] Parkin DM, Bray F, Ferlay J and Pisani P. Global cancer statistics, 2002. CA Cancer J Clin 2005; 55: 74-108.

[3] Jemal A, Siegel R, Ward E, Hao Y, Xu J and Thun MJ. Cancer statistics, 2009. CA Cancer J Clin 2009; 59: 225-249.

[4] NCCN. Clinical practice guidelines in oncology: non-small cell lung cancer. NCCN Clinical Practice Guidelines in Oncology, v2 2009.

[5] Borczuk AC, Toonkel RL and Powell CA. Genomics of lung cancer. Proc Am Thorac Soc 2009; 6: 152-158.

[6] Borczuk AC, Powell CA. Expression profiling and lung cancer development. Proc Am Thorac Soc 2007; 4: 127-132.

[7] Govindan R, Page N, Morgensztern D, Read W, Tierney R, Vlahiotis A, Spitznagel EL and Piccirillo J. Changing epidemiology of small-cell lung cancer in the United States over the last 30 years: analysis of the surveillance, epidemiologic, and end results database. J Clin Oncol 2006; 24: 4539-4543.

[8] Langer CJ, Besse B, Gulaberto A, Brambilla E and Soria JC. The evolving role of histology in

the management of advanced non-small cell lung cancer. J Clin Oncol 2010; 28: 5311-5320.
[9] Daraselia N, Yuryev A, Egorov S, Mazo I and Ispolatov I. Automatic extraction of gene ontology annotation and its correlation with clusters in protein network. BMC Bioinformatics 2007; 8: 243.
[10] Novichkova S, Egorov S and Daraselia N. MedScan, a natural language processing engine for MEDLINE abstracts. Bioinformatics 2011; 19: 1699-1706.
[11] Sivachenko AY, Yuryev A, Daraselia N and Mazo I. Molecular networks in microarray analysis. J Bioinform Comput Biol 2007; 5: 429-456.
[12] Sivachenko AY, Yuryev A, Daraselia N and Mazo I. Identifying local gene expression patterns in biomolecular networks, pp.180-184, 2005 IEE Computational Systems Bioinformatics Conference – Workshops (CSBW'05), 2005.
[13] Sivachenko AY, Kalinin A and Yuryev A. Pathway analysis for design of promiscuous drugs and selective drug mixtures. Curr Drug Discov Technol 2006; 3: 269-277.
[14] Yuryev A, Mulyukov Z, Kotelnikova E, Maslov S, Egorov S, Nikitin A, Daraselia N and Mazo I. Automatic pathway building in biological association networks. BMC Bioinformatics 2006; 7: 171.
[15] Yuryev A. In silico pathway analysis: the final frontier towards completely rational drug design. Expert Opinion Drug Discov 2008; 3: 867-876.
[16] Subramanian A, Tamayo P, Mootha VK, Mukherjee S, Ebert BL, Gillette MA, Paulovich A, Pomeroy SL, Golub TR, Lander ES and Mesirov JP. Gene set enrichment analysis; a knowledge-based approach for interpreting genome-wide expression profiles. Proc Natl Acad Sci USA 2005; 102: 15545-15550.
[17] Bracken CP, Gregory PA, Kolesnikoff N, Bert AG, Wang J, Shannon MF and Goodall GJ. A double-negative feedback loop between ZEB1-SIP1 and the microRNA-200 family regulates epithelial-mesenchymal transition. Cancer Res 2008; 68: 7846-7854.
[18] Wadehra M, Goodglick L and Braun J. The tetraspan protein EMP2 modulates the surface expression of caveolins and glycosylphosphatidyl inositol-linked proteins. Mol Biol Cell 2004; 15: 2073-2083.
[19] Wood RD, Mitchell M, Lindhal T. Human DNA repair genes, 2005. Mutat Res 2005; 577: 275-283.
[20] Chen PP, Li WJ, Wang Y, Zhao S, Li DY, Feng LY, Shi XL, Koeffler HP, Tong XJ and Xie D. Expression of Cyr61, CTGF and WISP-1 correlates with clinical features of lung cancer. PLoS ONE 2007; 2: e534.
[21] Donnem T, Al Saad S, Al Shibli K, Busund LT and Bremnes RM. Co-expression of PDGF-B and VEGFR-3 strongly correlates with lymph node metastasis and poor survival in non-small-cell lung cancer. Ann Oncol 2010; 21: 223-231.
[22] Kinoshita K, Nakagawa K, Hamada J, Hida Y, Tada M, Kondo S and Moriuchi T. Imatinib mesylate inhibits the proliferation-stimulating effect of human lung cancer-associated stromal fibroblasts on lung cancer cells. Int J Oncol 2010; 37: 869-877.

Supplementary material

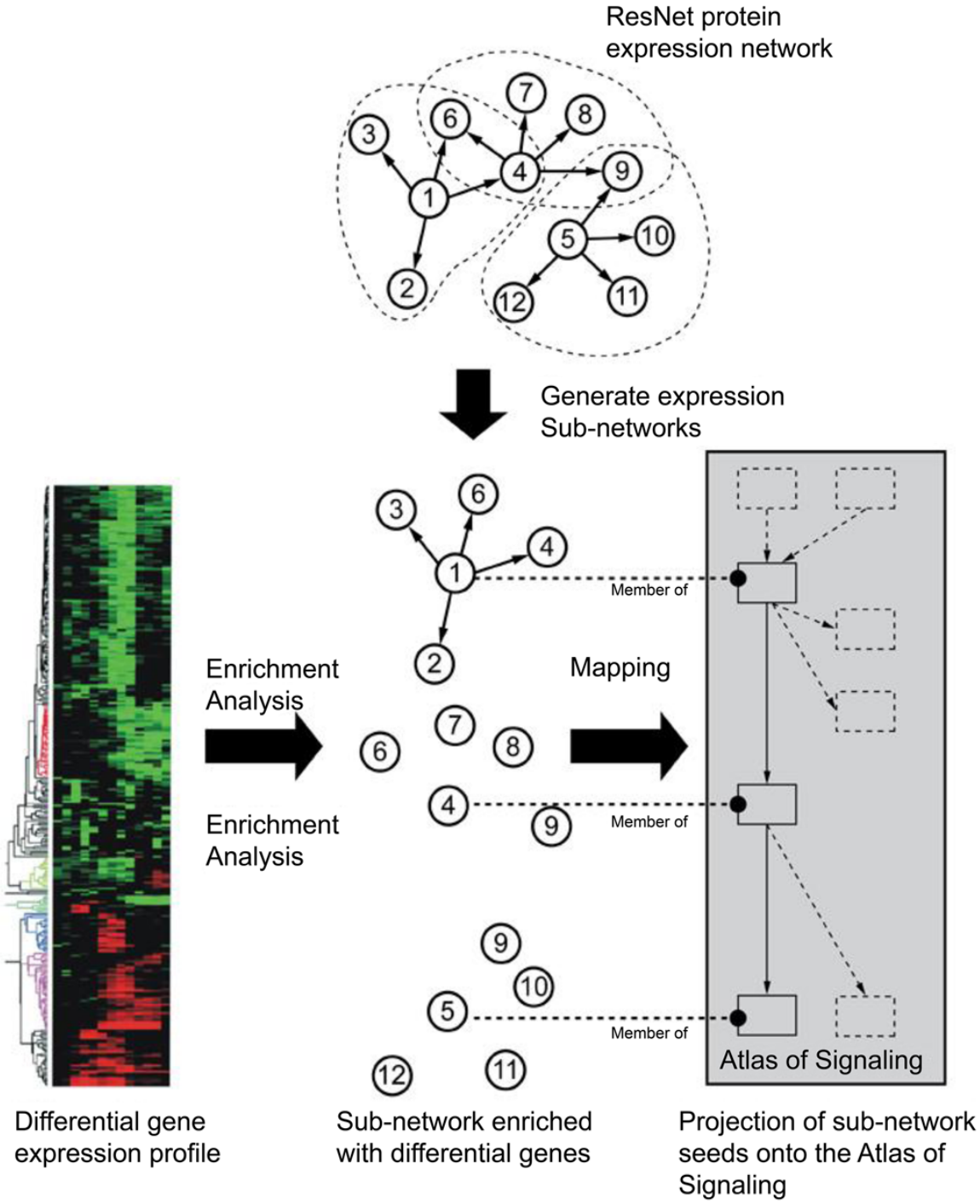

Figure S1. An overview of Sub-Network Enrichment Analysis (SNEA) algorithms

Table S1. Differential expression in DNA repair genes

Name	Description	SCC		ADC	
		fold-change	p-value	fold-change	p-value
RBBP8	Retinoblastoma binding protein 8	2.15	9.61×10^{-7}	1.26	5.34×10^{-2}
PRKDC	Protein kinase, DNA-activated, catalytic polypeptide	2.14	3.89×10^{-7}	1.45	1.10×10^{-3}
SHFM1	Split hand/foot malformation (ectrodactyly) type 1	2.12	1.96×10^{-7}	1.34	1.61×10^{-1}
PCNA	Proliferating cell nuclear antigen	2.01	1.66×10^{-6}	1.43	4.79×10^{-4}
CHEK1	CHK1 checkpoint homolog (*S. Pombe*)	1.97	1.33×10^{-5}	1.35	1.20×10^{-4}
FANCI	Fanconi anemia, complementation group I	1.84	2.79×10^{-6}	1.29	4.88×10^{-3}
CHAF1A	Chromatin assembly factor 1, subunit A (p150)	1.82	2.55×10^{-7}	1.28	1.52×10^{-4}
EXO1	Exonuclease 1	1.79	7.13×10^{-7}	1.36	4.29×10^{-4}
CHEK2	CHK2 checkpoint homolog *(S. Pombe*)	1.73	9.38×10^{-6}	1.18	1.62×10^{-2}
APEX1	APEX nuclease (multifunctional DNA repair enzyme) 1	1.73	6.67×10^{-7}	1.32	2.22×10^{-2}
BLM	Bloom syndrome, RecQ helicase-like	1.72	8.70×10^{-6}	1.25	1.41×10^{-4}
POLB	Polymerase (DNA directed), beta	1.59	8.74×10^{-5}	1.28	3.57×10^{-2}
BRCA1	Breast cancer 1, early onset	1.56	2.13×10^{-5}	1.11	1.25×10^{-1}
PMS2	PMS2 postmeiotic segregation increased 2 (*S. cerevisiae*)	1.54	3.87×10^{-4}	1.21	2.58×10^{-2}
PARP1	Poly (ADP-ribose) polymerase 1	1.54	3.11×10^{-4}	1.23	4.17×10^{-2}
CETN2	Centrin, EF-hand protein, 2	1.52	3.31×10^{-3}	-1.06	7.41×10^{-1}
CDK7	Cyclin-dependent kinase 7	1.50	1.53×10^{-4}	1.09	3.01×10^{-1}
MSH6	mutS homolog 6 (*E. Coli*)	1.49	1.29×10^{-3}	1.05	6.09×10^{-1}
ATR	Ataxia telangiectasia and Rad3 related	1.46	1.50×10^{-4}	1.10	2.66×10^{-1}
UBE2V2	Ubiquitin-conjugating enzyme E2 variant 2	1.45	2.00×10^{-5}	1.11	1.28×10^{-1}

FEN1	Flap structure-specific endonuclease 1	1.45	4.79×10^{-7}	1.39	4.18×10^{-7}
PARP2	Poly (ADP-ribose) polymerase 2	1.44	2.05×10^{-3}	1.06	5.74×10^{-1}
FANCD2	Fanconi anemia, complementation group D2	1.44	6.33×10^{-6}	1.09	1.90×10^{-1}
FANCL	Fanconi anemia, complementation group L	1.41	3.93×10^{-2}	-1.08	5.57×10^{-1}
RAD54B	RAD54 homolog B (*S. cerevisiae*)	1.41	4.37×10^{-6}	1.15	4.16×10^{-3}
GTF2H3	General transcription factor IIH, polypeptide 3, 34 kDa	1.38	1.58×10^{-3}	1.19	3.65×10^{-3}
TDG	Thymine-DNA glycosylase	1.38	1.58×10^{-3}	1.16	5.83×10^{-2}
XRCC6	X-ray repair complementing defective repair in Chinese hamster cells 6	1.37	1.98×10^{-3}	1.07	3.63×10^{-1}
UNG	Uracil-DNA glycosylase	1.36	1.67×10^{-5}	1.13	5.20×10^{-2}
MSH2	mutS homolog 2, colon cancer, nonpolyposis type 1 (*E. Coli*)	1.36	9.78×10^{-3}	1.26	1.49×10^{-3}
DDB1	Damage-specific DNA binding protein 1, 127 kDa	1.36	2.18×10^{-3}	1.12	2.29×10^{-1}
OBFC2B	Oligonucleotide/oligosaccharide-binding fold containing 2B	1.35	1.63×10^{-4}	1.15	9.60×10^{-3}
XRCC4	X-ray repair complementing defective repair in Chinese hamster cells 4	1.34	3.81×10^{-3}	1.13	1.12×10^{-1}
TDP1	Tyrosyl-DNA phosphodiesterase 1	1.29	1.75×10^{-4}	1.13	2.73×10^{-2}
PALB2	Partner and localizer of BRCA2	1.28	1.88×10^{-3}	1.05	3.43×10^{-1}
GTF2H1	General transcription factor IIH, polypeptide 1, 62 kDa	1.27	5.39×10^{-2}	1.13	1.53×10^{-1}
PMS2L3	Postmeiotic segregation increased 2-like 3	1.27	2.48×10^{-2}	1.28	1.76×10^{-2}
APTX	Aprataxin	1.26	2.40×10^{-3}	1.09	1.33×10^{-1}
MNAT1	Menage a trois homolog 1, cyclin H assembly factor (*X. laevis*)	1.26	1.54×10^{-2}	-1.01	8.98×10^{-1}
RAD51	RAD51 homolog (RecA homolog, *E. Coli*) (*S. cerevisiae*)	1.25	4.56×10^{-3}	1.14	2.94×10^{-2}
FANCF	Fanconi anemia,	1.24	3.57×10^{-3}	1.11	5.48×10^{-2}

	complementation group F				
DCLRE1A	DNA cross-link repair 1A (PSO2 homolog, *S. cerevisiae*)	1.24	2.93×10^{-3}	1.19	1.59×10^{-3}
RAD51C	RAD51 homolog C (*S. cerevisiae*)	1.24	3.84×10^{-3}	1.06	3.43×10^{-1}
RECQL	RecQ protein-like (DNA helicase Q1-like)	1.24	3.15×10^{-2}	1.04	5.70×10^{-1}
WRN	Werner syndrome, RecQ helicase-like	1.23	7.64×10^{-2}	-1.28	1.76×10^{-3}
XRCC5	X-ray repair complementing defective repair in Chinese hamster cells 5 (double-strand-break rejoining)	1.22	2.27×10^{-2}	-1.02	8.53×10^{-1}
RAD18	RAD18 homolog (*S. cerevisiae*)	1.22	1.58×10^{-4}	1.12	1.57×10^{-2}
ERCC6	Excision repair cross-complementing rodent repair deficiency, complementation group 6	1.20	1.10×10^{-2}	-1.03	6.42×10^{-1}
POLQ	Polymerase (DNA directed), theta	1.20	1.45×10^{-2}	1.05	3.89×10^{-1}
CLK2	CDC-like kinase 2	1.19	6.15×10^{-3}	1.27	1.55×10^{-4}
FANCE	Fanconi anemia, complementation group E	1.18	4.80×10^{-3}	1.04	3.84×10^{-1}
FANCA	Fanconi anemia, complementation group A	1.18	2.57×10^{-3}	1.15	3.99×10^{-3}
NUDT1	nudix (nucleoside diphosphate linked moiety X)-type motif 1	1.18	1.23×10^{-3}	1.15	1.33×10^{-2}
DUT	Deoxyuridine triphosphatase	1.18	4.96×10^{-3}	1.08	2.18×10^{-1}
TP53	tumor protein p53	1.18	6.27×10^{-2}	1.09	1.88×10^{-1}
RAD54L	RAD54-like (*S. cerevisiae*)	1.18	5.95×10^{-3}	1.16	9.38×10^{-3}
EME1	Essential meiotic endonuclease 1 homolog 1 (*S. Pombe*)	1.17	2.57×10^{-3}	1.14	3.56×10^{-2}
ERCC1	Excision repair cross-complementing rodent repair deficiency, complementation group 1 (includes overlapping antisense sequence)	1.17	6.47×10^{-4}	1.03	5.51×10^{-1}
RAD23B	RAD23 homolog B (*S. cerevisiae*)	1.17	7.37×10^{-2}	1.09	2.50×10^{-1}
BRCA2	breast cancer 2, early onset	1.17	1.61×10^{-2}	1.02	6.07×10^{-1}

SMUG1	single-strand-selective monofunctional uracil-DNA glycosylase 1	1.16	1.41×10^{-2}	1.12	3.81×10^{-2}
MSH5	mutS homolog 5 (*E. Coli*)	1.16	2.48×10^{-3}	1.10	7.79×10^{-2}
NBN	Nibrin	1.16	2.26×10^{-1}	1.10	3.12×10^{-1}
FANCG	Fanconi anemia, complementation group G	1.16	5.29×10^{-4}	1.10	7.89×10^{-2}
LIG3	Ligase III, DNA, ATP-dependent	1.16	2.82×10^{-2}	1.15	6.57×10^{-3}
RAD1	RAD1 homolog (*S. Pombe*)	1.15	3.82×10^{-2}	1.14	5.71×10^{-2}
RAD50	RAD50 homolog (*S. cerevisiae*)	1.15	3.50×10^{-1}	-1.14	3.96×10^{-1}
FANCB	Fanconi anemia, complementation group B	1.14	4.52×10^{-2}	1.17	1.22×10^{-2}
DDB2	Damage-specific DNA binding protein 2, 48 kDa	1.14	3.45×10^{-2}	1.15	4.07×10^{-3}
GTF2H5	General transcription factor IIH, polypeptide 5	1.14	7.73×10^{-2}	1.11	2.18×10^{-1}
RAD23A	RAD23 homolog A (*S. cerevisiae*)	1.13	1.05×10^{-1}	1.03	6.54×10^{-1}
POLE	Polymerase (DNA directed), epsilon	1.12	2.41×10^{-2}	1.05	3.21×10^{-1}
XRCC1	X-ray repair complementing defective repair in Chinese hamster cells 1	1.11	3.77×10^{-2}	1.13	2.74×10^{-3}
MRE11A	MRE11 meiotic recombination 11 homolog A (*S. cerevisiae*)	1.10	4.23×10^{-1}	1.05	6.12×10^{-1}
FANCM	Fanconi anemia, complementation group M	1.10	7.10×10^{-2}	-1.02	6.83×10^{-1}
APEX2	APEX nuclease (apurinic/apyrimidinic endonuclease) 2	1.10	5.71×10^{-2}	1.05	2.46×10^{-1}
PMS1	PMS1 postmeiotic segregation increased 1 (*S. cerevisiae*)	1.10	7.01×10^{-2}	1.09	6.87×10^{-2}
LIG1	Ligase I, DNA, ATP-dependent	1.09	4.08×10^{-2}	1.12	5.11×10^{-3}
NEIL3	nei endonuclease VIII-like 3 (*E. Coli*)	1.09	9.13×10^{-2}	1.12	6.20×10^{-2}
RPA1	Replication protein A1, 70 kDa	1.08	2.72×10^{-2}	1.08	4.27×10^{-2}
ALKBH2	alkB, alkylation repair homolog 2	1.08	1.96×10^{-1}	1.02	7.80×10^{-1}

	(*E. Coli*)				
ALKBH3	alkB, alkylation repair homolog 3 (*E. Coli*)	1.08	1.79×10^{-1}	1.08	2.22×10^{-1}
HUS1	HUS1 checkpoint homolog (*S. Pombe*)	1.08	2.59×10^{-1}	1.03	7.19×10^{-1}
UBE2A	Ubiquitin-conjugating enzyme E2A (RAD6 homolog)	1.08	2.09×10^{-1}	-1.01	8.50×10^{-1}
ERCC4	Excision repair cross-complementing rodent repair deficiency, complementation group 4	1.07	2.51×10^{-1}	1.06	3.21×10^{-1}
MBD4	Methyl-CpG binding domain protein 4	1.07	4.14×10^{-1}	1.11	5.74×10^{-2}
MAD2L2	MAD2 mitotic arrest deficient-like 2 (yeast)	1.07	2.13×10^{-1}	1.12	3.10×10^{-2}
LIG4	Ligase IV, DNA, ATP-dependent	1.06	3.15×10^{-1}	1.11	7.92×10^{-2}
RAD52	RAD52 homolog (*S. cerevisiae*)	1.06	3.06×10^{-1}	-1.05	2.82×10^{-1}
MDC1	Mediator of DNA damage checkpoint 1	1.06	4.24×10^{-1}	1.03	6.25×10^{-1}
MUTYH	mutY homolog (*E. Coli*)	1.06	2.57×10^{-1}	1.05	3.47×10^{-1}
RPA3	Replication protein A3, 14 kDa	1.06	2.83×10^{-1}	1.14	5.66×10^{-3}
POLH	Polymerase (DNA directed), eta	1.06	4.73×10^{-1}	1.11	2.02×10^{-1}
POLN	Polymerase (DNA directed) nu	1.05	2.92×10^{-1}	1.12	1.98×10^{-2}
GTF2H4	General transcription factor IIH, polypeptide 4, 52 kDa	1.05	1.64×10^{-1}	1.06	2.92×10^{-1}
DCLRE1C	DNA cross-link repair 1C (PSO2 homolog, *S. cerevisiae*)	1.05	4.68×10^{-1}	1.20	1.05×10^{-3}
XAB2	XPA binding protein 2	1.04	4.75×10^{-1}	1.07	1.75×10^{-1}
H2AFX	H2A histone family, member X	1.04	4.13×10^{-1}	1.25	4.58×10^{-6}
ERCC3	Excision repair cross-complementing rodent repair deficiency, complementation group 3 (xeroderma pigmentosum group B complementing)	1.04	6.20×10^{-1}	-1.05	5.19×10^{-1}
RAD51L1	RAD51-like 1 (*S. cerevisiae*)	1.04	5.92×10^{-1}	1.06	3.94×10^{-1}
XRCC3	X-ray repair complementing defective repair in Chinese	1.04	4.91×10^{-1}	1.18	2.41×10^{-3}

	hamster cells 3				
RPA2	replication protein A2, 32 kDa	1.04	6.87×10^{-1}	1.02	8.38×10^{-1}
ATM	ataxia telangiectasia mutated	1.04	7.26×10^{-1}	-1.21	7.93×10^{-2}
RAD17	RAD17 homolog (*S. Pombe*)	1.04	6.98×10^{-1}	1.21	1.44×10^{-2}
REV1	REV1 homolog (*S. cerevisiae*)	1.03	6.98×10^{-1}	-1.09	2.49×10^{-1}
RAD51L3	RAD51-like 3 (*S. cerevisiae*)	1.03	5.07×10^{-1}	1.06	2.89×10^{-1}
UBE2B	Ubiquitin-conjugating enzyme E2B (RAD6 homolog)	1.03	6.85×10^{-1}	-1.20	7.78×10^{-2}
RDM1	RAD52 motif 1	1.02	6.46×10^{-1}	1.16	4.44×10^{-3}
MSH4	mutS homolog 4 (*E. Coli*)	1.02	7.35×10^{-1}	1.00	9.38×10^{-1}
RECQL4	RecQ protein-like 4	1.02	6.92×10^{-1}	1.12	3.02×10^{-2}
ERCC2	Excision repair cross-complementing rodent repair deficiency, complementation group 2	1.01	8.80×10^{-1}	1.18	8.45×10^{-4}
NTHL1	nth endonuclease III-like 1 (*E. Coli*)	1.00	9.79×10^{-1}	1.07	1.54×10^{-1}
POLM	Polymerase (DNA directed), mu	-1.00	9.79×10^{-1}	1.07	1.53×10^{-1}
MSH3	mutS homolog 3 (*E. Coli*)	-1.00	9.80×10^{-1}	-1.00	9.47×10^{-1}
ERCC5	Excision repair cross-complementing rodent repair deficiency, complementation group 5	-1.00	9.70×10^{-1}	-1.32	2.85×10^{-3}
EME2	Essential meiotic endonuclease 1 homolog 2 (*S. Pombe*)	-1.01	8.17×10^{-1}	-1.02	6.86×10^{-1}
PNKP	Polynucleotide kinase 3'-phosphatase	-1.01	7.46×10^{-1}	1.14	4.45×10^{-3}
XPA	Xeroderma pigmentosum, complementation group A	-1.01	8.65×10^{-1}	-1.08	2.43×10^{-1}
POLD1	Polymerase (DNA directed), delta 1, catalytic subunit 125 kDa	-1.02	7.40×10^{-1}	1.05	3.27×10^{-1}
TREX2	Three prime repair exonuclease 2	-1.02	6.83×10^{-1}	1.10	9.88×10^{-2}
POLL	Polymerase (DNA directed), lambda	-1.02	6.14×10^{-1}	1.03	6.11×10^{-1}
MMS19	MMS19 nucleotide excision repair	-1.02	5.25×10^{-1}	-1.03	4.03×10^{-1}

	homolog (*S. cerevisiae*)				
MPG	N-methylpurine-DNA glycosylase	-1.03	4.49×10^{-1}	1.11	2.26×10^{-3}
RAD9A	RAD9 homolog A (*S. Pombe*)	-1.03	5.52×10^{-1}	1.06	2.13×10^{-1}
TREX1	Three prime repair exonuclease 1	-1.03	4.99×10^{-1}	-1.06	2.04×10^{-1}
MUS81	MUS81 endonuclease homolog (*S. cerevisiae*)	-1.04	4.33×10^{-1}	1.10	3.02×10^{-2}
OGG1	8-oxoguanine DNA glycosylase	-1.05	3.02×10^{-1}	1.08	8.32×10^{-2}
RECQL5	RecQ protein-like 5	-1.05	2.99×10^{-1}	1.11	4.41×10^{-2}
POLI	Polymerase (DNA directed) iota	-1.05	6.10×10^{-1}	-1.12	3.06×10^{-1}
DCLRE1B	DNA cross-link repair 1B (PSO2 homolog, *S. cerevisiae*)	-1.06	4.75×10^{-1}	1.11	1.35×10^{-1}
DMC1	DMC1 dosage suppressor of mck1 homolog, meiosis-specific homologous recombination (yeast)	-1.06	2.82×10^{-1}	1.07	2.07×10^{-1}
NEIL2	nei like 2 (*E. Coli*)	-1.07	1.90×10^{-1}	1.11	3.17×10^{-2}
POLK	Polymerase (DNA directed) kappa	-1.07	5.64×10^{-1}	-1.24	3.58×10^{-2}
ERCC8	Excision repair cross-complementing rodent repair deficiency, complementation group 8	-1.09	1.59×10^{-1}	1.05	3.57×10^{-1}
MGMT	O-6-methylguanine-DNA methyltransferase	-1.09	8.14×10^{-2}	1.05	1.79×10^{-1}
UBE2N	Ubiquitin-conjugating enzyme E2N (UBC13 homolog, yeast)	-1.09	1.84×10^{-1}	-1.11	8.47×10^{-2}
GTF2H2	General transcription factor IIH, polypeptide 2, 44 kDa	-1.10	5.17×10^{-1}	-1.20	2.56×10^{-1}
Hel308	Helicase, POLQ-like	-1.11	1.45×10^{-1}	-1.05	3.62×10^{-1}
SPO11	SPO11 meiotic protein covalently bound to DSB homolog (*S. cerevisiae*)	-1.11	1.26×10^{-1}	1.01	7.93×10^{-1}
MLH1	mutL homolog 1, colon cancer, nonpolyposis type 2 (*E. Coli*)	-1.12	1.27×10^{-1}	-1.23	2.00×10^{-3}
POLG	polymerase (DNA directed), gamma	-1.12	1.54×10^{-2}	1.03	5.51×10^{-1}
RRM2B	Ribonucleotide reductase M2 B	-1.13	8.62×10^{-2}	1.09	2.92×10^{-1}

	(TP53 inducible)				
RPA4	Replication protein A4, 34 kDa	-1.14	2.69×10^{-2}	-1.11	4.93×10^{-2}
NEIL1	nei endonuclease VIII-like 1 (*E. Coli*)	-1.14	2.79×10^{-2}	-1.04	4.78×10^{-1}
XPC	Xeroderma pigmentosum, complementation group C	-1.14	2.71×10^{-2}	-1.11	1.05×10^{-1}
MLH3	mutL homolog 3 (*E. Coli*)	-1.16	1.25×10^{-2}	-1.10	1.44×10^{-1}
FANCC	Fanconi anemia, complementation group C	-1.21	3.49×10^{-3}	-1.14	2.08×10^{-2}
REV3L	REV3-like, catalytic subunit of DNA polymerase zeta (yeast)	-1.25	1.14×10^{-2}	-1.19	3.02×10^{-2}
PER1	Period homolog 1 (*Drosophila*)	-1.37	5.61×10^{-6}	-1.19	7.80×10^{-3}
CCNH	Cyclin H	-1.69	1.94×10^{-4}	-1.50	1.66×10^{-2}
A730011L01Rik	Hypothetical protein FLJ35220				
GEN1	Gen homolog 1, endonuclease (*Drosophila*)				
PMS2L4	Postmeiotic segregation increased 2-like 4 pseudogene				
ATRIP	ATR interacting protein				
XRCC2	X-ray repair complementing defective repair in Chinese hamster cells 2				
C19orf40	Chromosome 19 open reading frame 40				

Table S2. Differential changes in cell cycle genes

Name	Description	SCC		ADC	
		fold-change	p-value	fold-change	p-value
TOP2A	Topoisomerase (DNA) II alpha 170 kDa	5.43	1.23×10^{-11}	2.92	7.95×10^{-9}
CCNB1	Cyclin B1	2.75	6.97×10^{-8}	1.56	4.82×10^{-5}
MELK	Maternal embryonic leucine zipper kinase	2.67	1.75×10^{-7}	1.45	3.21×10^{-6}
MAD2L1	MAD2 mitotic arrest deficient-like 1 (yeast)	2.63	4.69×10^{-9}	1.38	2.05×10^{-4}
SFN	Stratifin	2.60	1.94×10^{-7}	1.43	1.28×10^{-5}
CDC6	Cell division cycle 6 homolog (*S. cerevisiae*)	2.54	3.24×10^{-9}	1.54	2.40×10^{-4}
ASPM	asp (abnormal spindle) homolog, microcephaly associated (*Drosophila*)	2.48	1.45×10^{-7}	1.57	7.97×10^{-5}
TOPBP1	Topoisomerase (DNA) II binding protein 1	2.02	5.03×10^{-6}	1.18	4.88×10^{-2}
CHEK1	CHK1 checkpoint homolog (*S. Pombe*)	1.97	1.33×10^{-5}	1.35	1.20×10^{-4}
CCNB2	Cyclin B2	1.93	1.69×10^{-6}	1.30	5.87×10^{-4}
CDC2	Cell division cycle 2, G1 to S and G2 to M	1.84	2.57×10^{-6}	1.37	7.20×10^{-5}
EZH2	Enhancer of zeste homolog 2 (*Drosophila*)	1.78	6.05×10^{-8}	1.24	8.23×10^{-3}
CHEK2	CHK2 checkpoint homolog (*S. Pombe*)	1.73	9.38×10^{-6}	1.18	1.62×10^{-2}
CDK4	Cyclin-dependent kinase 4	1.70	3.64×10^{-6}	1.34	3.85×10^{-3}
GMNN	Geminin, DNA replication inhibitor	1.65	1.07×10^{-4}	1.16	5.31×10^{-2}
NAE1	NEDD8 activating enzyme E1 subunit 1	1.59	1.64×10^{-3}	1.10	3.85×10^{-1}
BRCA1	Breast cancer 1, early onset	1.56	2.13×10^{-5}	1.11	1.25×10^{-1}
CDK6	Cyclin-dependent kinase 6	1.47	2.86×10^{-3}	-1.03	6.09×10^{-1}
ATR	Ataxia telangiectasia and Rad3	1.46	1.50×10^{-4}	1.10	2.66×10^{-1}

	related				
FANCD2	Fanconi anemia, complementation group D2	1.44	6.33×10^{-6}	1.09	1.90×10^{-1}
HDAC1	Histone deacetylase 1	1.44	1.11×10^{-3}	1.12	3.54×10^{-1}
MSH2	mutS homolog 2, colon cancer, nonpolyposis type 1 (*E. Coli*)	1.36	9.78×10^{-3}	1.26	1.49×10^{-3}
BIRC5	Baculoviral IAP repeat-containing 5	1.35	1.93×10^{-7}	1.26	1.52×10^{-4}
BARD1	BRCA1 associated RING domain 1	1.33	9.99×10^{-4}	-1.04	3.95×10^{-1}
CDKN2A	Cyclin-dependent kinase inhibitor 2A (melanoma, p16, inhibits CDK4)	1.32	2.06×10^{-2}	1.26	1.15×10^{-3}
RAD51	RAD51 homolog (RecA homolog, *E. Coli*) (*S. cerevisiae*)	1.25	4.56×10^{-3}	1.14	2.94×10^{-2}
TBPL1	TBP-like 1	1.23	1.50×10^{-2}	-1.07	3.51×10^{-1}
RINT1	RAD50 interactor 1	1.21	4.38×10^{-3}	1.03	5.78×10^{-1}
FANCA	Fanconi anemia, complementation group A	1.18	2.57×10^{-3}	1.15	3.99×10^{-3}
TP53	Tumor protein p53	1.18	6.27×10^{-2}	1.09	1.88×10^{-1}
CDC25A	Cell division cycle 25 homolog A (*S. Pombe*)	1.17	1.92×10^{-3}	1.05	5.00×10^{-1}
BRCA2	Breast cancer 2, early onset	1.17	1.61×10^{-2}	1.02	6.07×10^{-1}
NBN	Nibrin	1.16	2.26×10^{-1}	1.10	3.12×10^{-1}
RAD50	RAD50 homolog (*S. cerevisiae*)	1.15	3.50×10^{-1}	-1.14	3.96×10^{-1}
LIMK1	LIM domain kinase 1	1.15	1.34×10^{-3}	1.20	1.67×10^{-3}
MAPK14	Mitogen-activated protein kinase 14	1.14	2.18×10^{-1}	1.03	8.05×10^{-1}
TAOK1	TAO kinase 1	1.13	3.32×10^{-1}	-1.15	3.06×10^{-1}
CDK5	Cyclin-dependent kinase 5	1.12	6.26×10^{-2}	1.26	6.48×10^{-4}
TP53BP1	Tumor protein p53 binding protein 1	1.12	8.23×10^{-2}	1.02	8.03×10^{-1}
POLE	Polymerase (DNA directed), epsilon	1.12	2.41×10^{-2}	1.05	3.21×10^{-1}

MRE11A	MRE11 meiotic recombination 11 homolog A (*S. cerevisiae*)	1.10	4.23×10^{-1}	1.05	6.12×10^{-1}
ETV6	ets variant 6	1.10	3.89×10^{-1}	1.14	7.57×10^{-2}
E2F1	E2F transcription factor 1	1.08	7.91×10^{-2}	1.21	9.59×10^{-3}
HUS1	HUS1 checkpoint homolog (*S. Pombe*)	1.08	2.59×10^{-1}	1.03	7.19×10^{-1}
GADD45A	Growth arrest and DNA-damage-inducible, alpha	1.07	5.45×10^{-1}	-1.00	9.99×10^{-1}
CDC25B	Cell division cycle 25 homolog B (*S. Pombe*)	1.07	3.34×10^{-1}	1.06	4.34×10^{-1}
MDC1	Mediator of DNA damage checkpoint 1	1.06	4.24×10^{-1}	1.03	6.25×10^{-1}
TOP2B	topoisomerase (DNA) II beta 180 kDa	1.06	6.39×10^{-1}	-1.29	3.22×10^{-2}
UBA3	Ubiquitin-like modifier activating enzyme 3	1.05	5.31×10^{-1}	1.02	7.93×10^{-1}
TP73	Tumor protein p73	1.05	2.53×10^{-1}	1.06	1.64×10^{-1}
CDK2	Cyclin-dependent kinase 2	1.05	5.94×10^{-1}	-1.09	2.64×10^{-1}
DCLRE1C	DNA cross-link repair 1C (PSO2 homolog, *S. cerevisiae*)	1.05	4.68×10^{-1}	1.20	1.05×10^{-3}
H2AFX	H2A histone family, member X	1.04	4.13×10^{-1}	1.25	4.58×10^{-6}
ATM	ataxia telangiectasia mutated	1.04	7.26×10^{-1}	-1.21	7.93×10^{-2}
RAD17	RAD17 homolog (*S. Pombe*)	1.04	6.98×10^{-1}	1.21	1.44×10^{-2}
TRAF2	TNF receptor-associated factor 2	1.02	6.59×10^{-1}	1.06	1.34×10^{-1}
UIMC1	Ubiquitin interaction motif containing 1	1.02	7.46×10^{-1}	1.09	1.30×10^{-1}
MAPKAPK 2	Mitogen-activated protein kinase-activated protein kinase 2	1.01	7.91×10^{-1}	1.02	7.06×10^{-1}
CDC25C	Cell division cycle 25 homolog C (*S. Pombe*)	1.01	8.74×10^{-1}	1.08	1.72×10^{-1}
TERF1	Telomeric repeat binding factor (NIMA-interacting) 1	1.01	9.26×10^{-1}	-1.02	8.44×10^{-1}
HDAC4	Histone deacetylase 4	1.01	8.64×10^{-1}	1.02	5.65×10^{-1}

MAP2K2	Mitogen-activated protein kinase kinase 2	1.00	9.69×10^{-1}	1.19	8.11×10^{-3}
SPDYA	Speedy homolog A (Xenopus laevis)	-1.01	8.79×10^{-1}	1.09	9.73×10^{-2}
CEP164	Centrosomal protein 164 kDa	-1.01	8.19×10^{-1}	1.00	9.67×10^{-1}
CDKN1B	Cyclin-dependent kinase inhibitor 1B (p27, Kip1)	-1.01	9.27×10^{-1}	-1.09	3.39×10^{-1}
PPP5C	Protein phosphatase 5, catalytic subunit	-1.01	8.02×10^{-1}	1.05	2.05×10^{-1}
CDKN2B	Cyclin-dependent kinase inhibitor 2B (p15, inhibits CDK4)	-1.01	8.38×10^{-1}	1.20	3.78×10^{-3}
FAM175A	Family with sequence similarity 175, member A	-1.02	7.51×10^{-1}	-1.02	7.81×10^{-1}
RAD9A	RAD9 homolog A (*S. Pombe*)	-1.03	5.52×10^{-1}	1.06	2.13×10^{-1}
CDT1	Chromatin licensing and DNA replication factor 1	-1.03	6.54×10^{-1}	1.18	1.91×10^{-2}
HMGN1	High-mobility group nucleosome binding domain 1	-1.04	3.83×10^{-1}	1.18	5.14×10^{-3}
PPP2CB	Protein phosphatase 2 (formerly 2A), catalytic subunit, beta isoform	-1.06	6.49×10^{-1}	-1.30	2.75×10^{-2}
MCPH1	Microcephalin 1	-1.07	2.65×10^{-1}	-1.00	9.96×10^{-1}
MAPK1	Mitogen-activated protein kinase 1	-1.08	4.32×10^{-1}	-1.26	1.93×10^{-2}
BTG3	BTG family, member 3	-1.09	4.16×10^{-1}	-1.07	4.18×10^{-1}
MLH1	mutL homolog 1, colon cancer, nonpolyposis type 2 (*E. Coli*)	-1.12	1.27×10^{-1}	-1.23	2.00×10^{-3}
CCNG1	Cyclin G1	-1.14	2.93×10^{-1}	-1.01	9.02×10^{-1}
CDKN1A	Cyclin-dependent kinase inhibitor 1A (p21, Cip1)	-1.16	1.18×10^{-1}	1.01	9.32×10^{-1}
PPM1D	Protein phosphatase 1D magnesium-dependent, delta isoform	-1.20	9.29×10^{-3}	-1.04	3.42×10^{-1}
WEE1	WEE1 homolog (*S. Pombe*)	-1.21	3.05×10^{-1}	-1.25	2.52×10^{-1}
FANCC	Fanconi anemia, complementation group C	-1.21	3.49×10^{-3}	-1.14	2.08×10^{-2}

MAPK3	Mitogen-activated protein kinase 3	-1.23	1.58×10^{-4}	-1.08	2.10×10^{-1}
PTGS2	Prostaglandin-endoperoxide synthase 2 (prostaglandin G/H synthase and cyclooxygenase)	-1.72	1.98×10^{-2}	-1.39	5.63×10^{-2}
KLF4	Kruppel-like factor 4 (gut)	-2.31	1.83×10^{-9}	-2.54	5.38×10^{-11}
CAV1	Caveolin 1, caveolae protein, 22 kDa	-4.24	2.78×10^{-10}	-4.80	3.59×10^{-12}
ATRIP	ATR interacting protein				

Table S3. Differential changes in apoptosis genes

Name	Description	SCC		ADC	
		fold-change	p-value	fold-change	p-value
Bim	BCL2-like 11 (apoptosis facilitator)	1.56	6.19×10^{-6}	1.04	4.42×10^{-1}
CYCS	Cytochrome c, somatic	1.49	1.46×10^{-3}	1.10	4.69×10^{-1}
ATR	Ataxia telangiectasia and Rad3 related	1.46	1.50×10^{-4}	1.10	2.66×10^{-1}
CAPN1	Calpain 1, (mu/I) large subunit	1.42	1.09×10^{-7}	1.21	1.46×10^{-3}
BIK	BCL2-interacting killer (apoptosis-inducing)	1.38	4.47×10^{-6}	1.21	1.73×10^{-3}
CASP3	Caspase 3, apoptosis-related cysteine peptidase	1.37	1.95×10^{-4}	1.08	2.50×10^{-1}
BIRC5	Baculoviral IAP repeat-containing 5	1.35	1.93×10^{-7}	1.26	1.52×10^{-4}
BAG1	BCL2-associated athanogene	1.23	1.19×10^{-1}	-1.08	4.39×10^{-1}
BIRC4	X-linked inhibitor of apoptosis	1.22	1.26×10^{-2}	-1.01	9.11×10^{-1}
TP53	Tumor protein p53	1.18	6.27×10^{-2}	1.09	1.88×10^{-1}
DFFA	DNA fragmentation factor, 45 kDa, alpha polypeptide	1.18	2.40×10^{-2}	1.09	1.07×10^{-1}
AIFM1	Apoptosis-inducing factor, mitochondrion-associated, 1	1.15	5.22×10^{-2}	1.09	1.77×10^{-1}
BAK1	BCL2-antagonist/killer 1	1.13	1.08×10^{-1}	1.06	6.30×10^{-1}
ENDOG	Endonuclease G	1.12	5.69×10^{-3}	1.11	6.11×10^{-2}
BAX	BCL2-associated X protein	1.10	5.67×10^{-2}	1.21	4.78×10^{-4}
GZMK	Granzyme K (granzyme 3; tryptase II)	1.08	5.59×10^{-1}	-1.17	2.67×10^{-1}
DIABLO	Diablo homolog (*Drosophila*)	1.08	2.01×10^{-1}	1.09	1.01×10^{-1}
CASP6	Caspase 6, apoptosis-related cysteine peptidase	1.07	4.09×10^{-1}	1.16	7.90×10^{-2}
MDM2	Mdm2 p53 binding protein homolog (mouse)	1.05	5.56×10^{-1}	-1.04	8.03×10^{-1}

GZMB	Granzyme B (granzyme 2, cytotoxic T-lymphocyte-associated serine esterase 1)	1.05	6.19×10^{-1}	-1.18	1.08×10^{-3}
ATM	Ataxia telangiectasia mutated	1.04	7.26×10^{-1}	-1.21	7.93×10^{-2}
AKT1	v-akt murine thymoma viral oncogene homolog 1	1.03	6.06×10^{-1}	1.14	1.98×10^{-2}
BOK	BCL2-related ovarian killer	1.01	8.26×10^{-1}	1.11	6.98×10^{-2}
BID	BH3 interacting domain death agonist	1.01	8.65×10^{-1}	1.05	2.70×10^{-1}
BCL2L2	BCL2-like 2	1.01	9.44×10^{-1}	-1.12	1.09×10^{-1}
BMF	Bcl2 modifying factor	-1.00	9.97×10^{-1}	1.12	3.21×10^{-2}
BCL2L1	BCL2-like 1	-1.01	8.91×10^{-1}	-1.02	8.72×10^{-1}
BCL2	B-cell CLL/lymphoma 2	-1.04	4.97×10^{-1}	1.08	8.44×10^{-2}
CASP7	Caspase 7, apoptosis-related cysteine peptidase	-1.04	4.80×10^{-1}	1.02	7.05×10^{-1}
BBC3	BCL2 binding component 3	-1.05	3.36×10^{-1}	1.12	8.96×10^{-3}
DFFB	DNA fragmentation factor, 40 kDa, beta polypeptide (caspase-activated DNase)	-1.05	2.89×10^{-1}	1.03	6.72×10^{-1}
APAF1	Apoptotic peptidase activating factor 1	-1.05	2.49×10^{-1}	-1.04	3.48×10^{-1}
BCL2L10	BCL2-like 10 (apoptosis facilitator)	-1.06	2.93×10^{-1}	1.10	1.04×10^{-1}
CASP9	Caspase 9, apoptosis-related cysteine peptidase	-1.08	1.61×10^{-1}	1.04	4.76×10^{-1}
BIRC2	Baculoviral IAP repeat-containing 2	-1.11	1.48×10^{-1}	-1.30	6.32×10^{-3}
CASP10	Caspase 10, apoptosis-related cysteine peptidase	-1.12	1.46×10^{-1}	1.01	8.79×10^{-1}
BCL2A1	BCL2-related protein A1	-1.12	3.60×10^{-1}	-1.20	5.64×10^{-2}
CASP4	Caspase 4, apoptosis-related cysteine peptidase	-1.13	2.69×10^{-1}	-1.13	2.76×10^{-1}
BAD	BCL2-associated agonist of cell death	-1.14	2.46×10^{-2}	1.06	1.96×10^{-1}

CASP8	Caspase 8, apoptosis-related cysteine peptidase	-1.16	3.38×10^{-2}	-1.20	1.48×10^{-2}
NAIP	NLR family, apoptosis inhibitory protein	-1.23	2.90×10^{-2}	-1.17	6.10×10^{-2}
BIRC3	Baculoviral IAP repeat-containing 3	-1.27	1.25×10^{-1}	1.04	7.99×10^{-1}
CAPN2	Calpain 2, (m/II) large subunit	-1.41	2.71×10^{-4}	-1.22	1.81×10^{-1}
MCL1	Myeloid cell leukemia sequence 1 (BCL2-related)	-1.81	6.44×10^{-8}	-1.59	8.64×10^{-5}
CFLAR	CASP8 and FADD-like apoptosis regulator	-2.34	2.59×10^{-10}	-1.80	1.80×10^{-4}

Table S4. Differential changes in oncogenes

Name	Description	SCC		ADC	
		fold-change	p-value	fold-change	p-value
ECT2	Epithelial cell transforming sequence 2 oncogene	3.59	2.55×10^{-8}	1.54	4.55×10^{-3}
DCUN1D1	DCN1, defective in cullin neddylation 1, domain containing 1 (*S. cerevisiae*)	2.66	4.00×10^{-7}	-1.06	4.63×10^{-1}
RAB10	RAB10, member RAS oncogene family	1.84	2.24×10^{-5}	1.13	4.28×10^{-1}
RAB25	RAB25, member RAS oncogene family	1.65	2.09×10^{-4}	1.78	1.55×10^{-7}
MET	met proto-oncogene (hepatocyte growth factor receptor)	1.60	8.63×10^{-3}	1.51	3.08×10^{-2}
NAE1	NEDD8 activating enzyme E1 subunit 1	1.59	1.64×10^{-3}	1.10	3.85×10^{-1}
RAP2B	RAP2B, member of RAS oncogene family	1.56	9.39×10^{-5}	1.14	1.07×10^{-2}
MCM3	Minichromosome maintenance complex component 3	1.56	4.24×10^{-5}	1.20	3.48×10^{-2}
SLC4A1AP	Solute carrier family 4 (anion exchanger), member 1, adaptor protein	1.52	4.59×10^{-3}	1.05	7.03×10^{-1}
DEK	DEK oncogene	1.50	2.98×10^{-3}	-1.04	7.59×10^{-1}
RAB38	RAB38, member RAS oncogene family	1.49	4.24×10^{-4}	1.16	3.15×10^{-2}
HRASLS	HRAS-like suppressor	1.48	3.54×10^{-5}	1.36	1.94×10^{-4}
SET	SET nuclear oncogene	1.45	3.91×10^{-5}	1.06	5.01×10^{-1}
KRAS	v-Ki-ras2 Kirsten rat sarcoma viral oncogene homolog	1.45	1.11×10^{-3}	1.01	9.30×10^{-1}
NET1	Neuroepithelial cell transforming 1	1.42	2.25×10^{-4}	1.38	4.58×10^{-5}
P4HB	Prolyl 4-hydroxylase, beta polypeptide	1.42	5.22×10^{-5}	1.45	1.69×10^{-3}
EIF3E	Eukaryotic translation initiation factor 3, subunit E	1.41	6.90×10^{-3}	1.13	3.06×10^{-1}

PARK7	Parkinson disease (autosomal recessive, early onset) 7	1.40	4.04×10^{-4}	1.31	9.36×10^{-3}
TFG	TRK-fused gene	1.39	1.12×10^{-2}	1.21	3.35×10^{-2}
MYBL2	v-myb myeloblastosis viral oncogene homolog (avian)-like 2	1.38	4.82×10^{-7}	1.21	2.09×10^{-3}
MYC	v-myc myelocytomatosis viral oncogene homolog (avian)	1.36	5.01×10^{-2}	-1.21	4.14×10^{-2}
CRKL	v-crk sarcoma virus CT10 oncogene homolog (avian)-like	1.36	8.49×10^{-6}	1.10	1.41×10^{-1}
CTTN	Cortactin	1.35	1.90×10^{-2}	1.22	8.26×10^{-2}
GNB2L1	Guanine nucleotide binding protein (G protein), beta polypeptide 2-like 1	1.32	6.89×10^{-3}	1.04	7.48×10^{-1}
LCN2	Lipocalin 2	1.31	2.80×10^{-2}	-1.00	9.66×10^{-1}
RAN	RAN, member RAS oncogene family	1.31	3.58×10^{-6}	1.28	3.71×10^{-6}
RAB18	RAB18, member RAS oncogene family	1.30	8.31×10^{-2}	-1.13	3.36×10^{-1}
BMI1	BMI1 polycomb ring finger oncogene	1.29	1.26×10^{-2}	1.03	8.21×10^{-1}
RAB30	RAB30, member RAS oncogene family	1.28	8.22×10^{-3}	1.12	1.69×10^{-1}
RAB11A	RAB11A, member RAS oncogene family	1.28	8.28×10^{-2}	-1.41	7.79×10^{-3}
RAB13	RAB13, member RAS oncogene family	1.26	3.18×10^{-2}	1.19	2.55×10^{-1}
RAB6B	RAB6B, member RAS oncogene family	1.26	5.74×10^{-3}	1.11	1.84×10^{-3}
YES1	v-yes-1 Yamaguchi sarcoma viral oncogene homolog 1	1.25	3.59×10^{-2}	-1.04	6.83×10^{-1}
PIM2	pim-2 oncogene	1.24	5.84×10^{-3}	1.23	1.27×10^{-3}
ARHGEF5	Rho guanine nucleotide exchange factor (GEF) 5	1.24	1.80×10^{-2}	1.05	4.13×10^{-1}
MYB	v-myb myeloblastosis viral oncogene homolog (avian)	1.24	4.77×10^{-2}	-1.01	9.21×10^{-1}

HRAS	v-Ha-ras Harvey rat sarcoma viral oncogene homolog	1.23	1.95×10^{-5}	1.19	6.43×10^{-5}
RAB15	RAB15, member RAS onocogene family	1.23	4.39×10^{-3}	1.13	4.13×10^{-2}
EGFR	Epidermal growth factor receptor (erythroblastic leukemia viral (v-erb-b) oncogene homolog, avian)	1.22	1.90×10^{-2}	1.30	1.06×10^{-1}
RAB22A	RAB22A, member RAS oncogene family	1.21	8.18×10^{-3}	1.17	4.41×10^{-2}
TPR	Translocated promoter region (to activated MET oncogene)	1.19	1.23×10^{-1}	-1.04	7.82×10^{-1}
NRAS	Neuroblastoma RAS viral (v-ras) oncogene homolog	1.19	4.03×10^{-2}	1.11	1.30×10^{-1}
RAB9A	RAB9A, member RAS oncogene family	1.18	7.47×10^{-2}	1.03	7.55×10^{-1}
FGFR1OP	FGFR1 oncogene partner	1.18	2.39×10^{-3}	1.01	8.26×10^{-1}
NUP214	Nucleoporin 214 kDa	1.18	3.40×10^{-2}	-1.19	2.16×10^{-2}
RALA	v-ral simian leukemia viral oncogene homolog A (ras related)	1.17	5.29×10^{-2}	1.02	8.17×10^{-1}
FGFR1OP 2	FGFR1 oncogene partner 2	1.17	1.84×10^{-1}	1.04	7.76×10^{-1}
EWSR1	Ewing sarcoma breakpoint region 1	1.17	4.91×10^{-2}	-1.09	2.18×10^{-1}
RAB1A	RAB1A, member RAS oncogene family	1.17	2.81×10^{-1}	1.07	6.85×10^{-1}
MAFB	v-maf musculoaponeurotic fibrosarcoma oncogene homolog B (avian)	1.16	9.99×10^{-2}	1.04	5.73×10^{-1}
RUNX1	runt-related transcription factor 1	1.16	3.46×10^{-2}	1.23	3.37×10^{-4}
RAB2A	RAB2A, member RAS oncogene family	1.16	1.31×10^{-1}	1.13	2.68×10^{-1}
FUS	Fusion (involved in t(12;16) in malignant liposarcoma)	1.16	1.21×10^{-1}	-1.02	8.58×10^{-1}
RAB3B	RAB3B, member RAS oncogene family	1.15	9.92×10^{-2}	1.19	3.84×10^{-2}
AKT2	v-akt murine thymoma viral	1.14	9.05×10^{-3}	1.01	8.07×10^{-1}

	oncogene homolog 2				
RAB27B	RAB27B, member RAS oncogene family	1.14	1.22×10^{-1}	1.10	2.80×10^{-1}
HKR1	GLI-Kruppel family member HKR1	1.14	5.99×10^{-2}	1.11	1.08×10^{-2}
ITPA	Inosine triphosphatase (nucleoside triphosphate pyrophosphatase)	1.13	2.09×10^{-2}	1.09	6.25×10^{-2}
MYCL1	v-myc myelocytomatosis viral oncogene homolog 1, lung carcinoma derived (avian)	1.13	1.19×10^{-2}	1.18	1.35×10^{-2}
MERTK	c-mer proto-oncogene tyrosine kinase	1.13	2.82×10^{-1}	1.03	7.69×10^{-1}
BRI3BP	BRI3 binding protein	1.13	5.26×10^{-2}	1.23	4.03×10^{-4}
ENTPD5	ectonucleoside triphosphate diphosphohydrolase 5	1.13	1.89×10^{-1}	1.11	1.60×10^{-1}
RAB1B	RAB1B, member RAS oncogene family	1.12	2.26×10^{-1}	1.07	5.58×10^{-1}
SKIL	SKI-like oncogene	1.12	3.14×10^{-1}	-1.05	6.63×10^{-1}
RAB7A	RAB7A, member RAS oncogene family	1.12	2.95×10^{-1}	-1.27	1.11×10^{-1}
RAB40C	RAB40C, member RAS oncogene family	1.11	8.23×10^{-2}	1.32	1.24×10^{-4}
RAB12	RAB12, member RAS oncogene family	1.11	4.32×10^{-2}	-1.03	5.35×10^{-1}
IRF4	Interferon regulatory factor 4	1.11	1.93×10^{-1}	1.10	2.44×10^{-2}
ELK1	ELK1, member of ETS oncogene family	1.10	4.22×10^{-2}	1.15	6.63×10^{-3}
ETV6	ets variant 6	1.10	3.89×10^{-1}	1.14	7.57×10^{-2}
RAB40B	RAB40B, member RAS oncogene family	1.10	5.42×10^{-2}	1.15	1.38×10^{-3}
TET1	tet oncogene 1	1.10	2.30×10^{-1}	1.03	5.79×10^{-1}
RAB8A	RAB8A, member RAS oncogene family	1.08	4.70×10^{-1}	-1.26	1.09×10^{-1}
RABL4	RAB, member of RAS oncogene family-like 4	1.08	2.30×10^{-1}	1.12	8.22×10^{-2}

BLOC1S2	Biogenesis of lysosomal organelles complex-1, subunit 2	1.08	3.59×10^{-1}	1.01	8.43×10^{-1}
RAB3D	RAB3D, member RAS oncogene family	1.08	1.95×10^{-1}	1.08	2.11×10^{-1}
VAV2	vav 2 guanine nucleotide exchange factor	1.08	3.26×10^{-1}	1.01	8.41×10^{-1}
RAB7L1	RAB7, member RAS oncogene family-like 1	1.07	1.27×10^{-1}	-1.08	1.81×10^{-1}
MRPS11	Mitochondrial ribosomal protein S11	1.07	1.84×10^{-1}	1.17	5.48×10^{-3}
CBL	Cas-Br-M (murine) ecotropic retroviral transforming sequence	1.07	1.83×10^{-1}	-1.03	5.84×10^{-1}
RAP2C	RAP2C, member of RAS oncogene family	1.07	2.09×10^{-1}	1.15	8.69×10^{-4}
RAB6A	RAB6A, member RAS oncogene family	1.07	4.65×10^{-1}	1.01	8.62×10^{-1}
RAB23	RAB23, member RAS oncogene family	1.07	5.96×10^{-1}	-1.32	2.63×10^{-2}
RAB3A	RAB3A, member RAS oncogene family	1.06	1.36×10^{-1}	1.10	7.76×10^{-2}
RAB21	RAB21, member RAS oncogene family	1.06	6.12×10^{-1}	-1.23	1.99×10^{-1}
TMEM50A	Transmembrane protein 50A	1.06	6.51×10^{-1}	-1.06	5.98×10^{-1}
RELB	v-rel reticuloendotheliosis viral oncogene homolog B	1.05	3.13×10^{-1}	1.12	6.33×10^{-2}
RAB26	RAB26, member RAS oncogene family	1.05	3.25×10^{-1}	1.21	1.53×10^{-3}
GLI3	GLI family zinc finger 3	1.05	5.64×10^{-1}	-1.03	6.47×10^{-1}
GLI4	GLI family zinc finger 4	1.04	4.00×10^{-1}	1.14	5.81×10^{-4}
RRAS2	Related RAS viral (r-ras) oncogene homolog 2	1.04	4.13×10^{-1}	1.20	1.64×10^{-4}
NR2F6	Nuclear receptor subfamily 2, group F, member 6	1.04	4.42×10^{-1}	1.23	4.71×10^{-5}
FGF3	Fibroblast growth factor 3 (murine mammary tumor virus integration site (v-int-2) oncogene homolog)	1.04	4.62×10^{-1}	1.21	1.62×10^{-2}

PIM1	pim-1 oncogene	1.04	6.53×10^{-1}	1.07	1.13×10^{-1}
ZSCAN22	Zinc finger and SCAN domain containing 22	1.03	5.80×10^{-1}	1.06	2.53×10^{-1}
DDX6	DEAD (Asp-Glu-Ala-Asp) box polypeptide 6	1.03	8.35×10^{-1}	-1.18	2.93×10^{-1}
RAB35	RAB35, member RAS oncogene family	1.03	7.65×10^{-1}	-1.09	3.27×10^{-1}
ELK4	ELK4, ETS-domain protein (SRF accessory protein 1)	1.03	5.53×10^{-1}	-1.09	8.34×10^{-2}
AKT1	v-akt murine thymoma viral oncogene homolog 1	1.03	6.06×10^{-1}	1.14	1.98×10^{-2}
RAB28	RAB28, member RAS oncogene family	1.03	7.67×10^{-1}	-1.13	3.06×10^{-1}
ERBB3	v-erb-b2 erythroblastic leukemia viral oncogene homolog 3 (avian)	1.03	6.41×10^{-1}	1.22	2.29×10^{-4}
ARAF	v-raf murine sarcoma 3611 viral oncogene homolog	1.03	6.08×10^{-1}	1.10	2.20×10^{-2}
ETV7	ets variant 7	1.03	6.19×10^{-1}	-1.01	8.07×10^{-1}
RAB34	RAB34, member RAS oncogene family	1.03	5.98×10^{-1}	1.24	1.77×10^{-6}
MAFG	v-maf musculoaponeurotic fibrosarcoma oncogene homolog G (avian)	1.02	5.43×10^{-1}	1.04	2.90×10^{-1}
RAB14	RAB14, member RAS oncogene family	1.02	8.66×10^{-1}	-1.57	3.44×10^{-3}
RAB3C	RAB3C, member RAS oncogene family	1.02	7.84×10^{-1}	-1.05	4.08×10^{-1}
MAF	v-maf musculoaponeurotic fibrosarcoma oncogene homolog (avian)	1.02	7.34×10^{-1}	-1.13	2.73×10^{-3}
RAB39B	RAB39B, member RAS oncogene family	1.02	7.28×10^{-1}	-1.02	7.92×10^{-1}
RET	ret proto-oncogene	1.02	6.56×10^{-1}	1.01	8.71×10^{-1}
RALB	v-ral simian leukemia viral oncogene homolog B (ras related; GTP binding protein)	1.02	8.65×10^{-1}	-1.35	8.13×10^{-3}

SRC	v-src sarcoma (Schmidt-Ruppin A-2) viral oncogene homolog (avian)	1.02	6.52×10^{-1}	1.10	2.50×10^{-2}
TTC23	Tetratricopeptide repeat domain 23	1.02	7.68×10^{-1}	-1.03	4.95×10^{-1}
WNT3	Wingless-type MMTV integration site family, member 3	1.02	7.43×10^{-1}	1.20	5.90×10^{-4}
GLI1	GLI family zinc finger 1	1.02	7.63×10^{-1}	1.12	7.94×10^{-2}
GLI2	GLI family zinc finger 2	1.02	7.61×10^{-1}	1.11	3.29×10^{-2}
MAFA	v-maf musculoaponeurotic fibrosarcoma oncogene homolog A (avian)	1.01	8.88×10^{-1}	1.15	8.23×10^{-3}
RHOC	ras homolog gene family, member C	1.01	9.24×10^{-1}	1.08	2.34×10^{-1}
RAB24	RAB24, member RAS oncogene family	1.01	8.90×10^{-1}	1.06	1.48×10^{-1}
RAB33B	RAB33B, member RAS oncogene family	1.01	9.39×10^{-1}	1.11	1.03×10^{-1}
EPHA1	EPH receptor A1	1.00	8.99×10^{-1}	1.08	7.17×10^{-2}
RAB5B	RAB5B, member RAS oncogene family	1.00	9.91×10^{-1}	-1.11	3.12×10^{-1}
WNT1	Wingless-type MMTV integration site family, member 1	1.00	9.91×10^{-1}	1.13	2.91×10^{-2}
CRK	v-crk sarcoma virus CT10 oncogene homolog (avian)	-1.00	9.49×10^{-1}	1.06	3.64×10^{-1}
TCL1A	T-cell leukemia/lymphoma 1A	-1.00	9.51×10^{-1}	1.12	5.70×10^{-2}
RABL5	RAB, member RAS oncogene family-like 5	-1.01	9.11×10^{-1}	1.05	3.03×10^{-1}
RAB33A	RAB33A, member RAS oncogene family	-1.01	8.79×10^{-1}	1.08	2.20×10^{-1}
RAB5C	RAB5C, member RAS oncogene family	-1.01	9.07×10^{-1}	1.07	4.51×10^{-1}
MCF2	MCF.2 cell line derived transforming sequence	-1.01	8.35×10^{-1}	1.13	2.25×10^{-2}
MYCN	v-myc myelocytomatosis viral related oncogene, neuroblastoma derived (avian)	-1.01	8.23×10^{-1}	1.16	1.08×10^{-2}

ABL2	v-abl Abelson murine leukemia viral oncogene homolog 2 (arg, Abelson-related gene)	-1.01	8.34×10^{-1}	1.09	5.15×10^{-2}
FGF4	Fibroblast growth factor 4	-1.01	7.91×10^{-1}	1.13	1.70×10^{-2}
SSPN	Sarcospan (Kras oncogene-associated gene)	-1.01	8.01×10^{-1}	1.00	9.41×10^{-1}
MOS	v-mos Moloney murine sarcoma viral oncogene homolog	-1.02	8.30×10^{-1}	1.03	6.99×10^{-1}
RAB11B	RAB11B, member RAS oncogene family	-1.02	8.33×10^{-1}	-1.04	4.85×10^{-1}
RAB2B	RAB2B, member RAS oncogene family	-1.02	8.57×10^{-1}	-1.17	9.91×10^{-2}
ERAS	ES cell expressed Ras	-1.02	7.42×10^{-1}	1.13	1.49×10^{-2}
RGL2	ral guanine nucleotide dissociation stimulator-like 2	-1.02	7.53×10^{-1}	1.00	9.86×10^{-1}
RAB4B	RAB4B, member RAS oncogene family	-1.02	6.15×10^{-1}	1.06	2.23×10^{-1}
RABL3	RAB, member of RAS oncogene family-like 3	-1.02	8.66×10^{-1}	1.04	7.08×10^{-1}
RAB7B	RAB7B, member RAS oncogene family	-1.02	5.44×10^{-1}	1.02	5.34×10^{-1}
LCK	Lymphocyte-specific protein tyrosine kinase	-1.03	6.40×10^{-1}	1.06	2.08×10^{-1}
FEV	FEV (ETS oncogene family)	-1.03	6.62×10^{-1}	1.18	5.08×10^{-3}
RAB5A	RAB5A, member RAS oncogene family	-1.03	7.21×10^{-1}	-1.04	7.41×10^{-1}
NTRK1	Neurotrophic tyrosine kinase, receptor, type 1	-1.03	5.13×10^{-1}	1.09	7.97×10^{-2}
MMEL1	Membrane metallo-endopeptidase-like 1	-1.03	5.53×10^{-1}	1.07	1.92×10^{-1}
THPO	Thrombopoietin	-1.03	5.85×10^{-1}	1.04	4.43×10^{-1}
CALCA	Calcitonin-related polypeptide alpha	-1.03	5.76×10^{-1}	1.25	2.73×10^{-1}
BCL2	B-cell CLL/lymphoma 2	-1.04	4.97×10^{-1}	1.08	8.44×10^{-2}
CCND1	cyclin D1	-1.04	6.52×10^{-1}	1.06	4.94×10^{-1}

ELK3	ELK3, ETS-domain protein (SRF accessory protein 2)	-1.04	6.50×10^{-1}	1.00	9.81×10^{-1}
TLX1	T-cell leukemia homeobox 1	-1.04	6.24×10^{-1}	1.05	3.92×10^{-1}
ERBB2	v-erb-b2 erythroblastic leukemia viral oncogene homolog 2, neuro/glioblastoma derived oncogene homolog (avian)	-1.04	5.39×10^{-1}	1.12	1.47×10^{-2}
RELA	v-rel reticuloendotheliosis viral oncogene homolog A (avian)	-1.04	4.91×10^{-1}	-1.01	8.22×10^{-1}
RAB6C	RAB6C, member RAS oncogene family	-1.04	6.76×10^{-1}	-1.25	1.04×10^{-1}
RAB36	RAB36, member RAS oncogene family	-1.05	3.46×10^{-1}	-1.09	7.18×10^{-2}
MAS1L	MAS1 oncogene-like	-1.05	4.83×10^{-1}	1.04	5.47×10^{-1}
RAB32	RAB32, member RAS oncogene family	-1.05	3.54×10^{-1}	1.11	5.44×10^{-2}
RAB39	RAB39, member RAS oncogene family	-1.05	4.87×10^{-1}	1.04	5.47×10^{-1}
MPL	Myeloproliferative leukemia virus oncogene	-1.06	1.56×10^{-1}	-1.02	5.97×10^{-1}
RAB43	RAB43, member RAS oncogene family	-1.06	4.88×10^{-1}	-1.00	9.83×10^{-1}
RAB40AL	RAB40A, member RAS oncogene family-like	-1.07	4.55×10^{-1}	1.02	7.75×10^{-1}
RAP2A	RAP2A, member of RAS oncogene family	-1.07	4.17×10^{-1}	-1.00	9.80×10^{-1}
FOXG1	Forkhead box G1	-1.07	1.79×10^{-1}	1.16	1.04×10^{-2}
RAB9B	RAB9B, member RAS oncogene family	-1.08	1.73×10^{-1}	-1.02	7.98×10^{-1}
TCL1B	T-cell leukemia/lymphoma 1B	-1.08	1.63×10^{-1}	1.11	1.35×10^{-1}
RAB41	RAB41, member RAS oncogene family	-1.08	1.18×10^{-1}	1.02	8.04×10^{-1}
MAFK	v-maf musculoaponeurotic fibrosarcoma oncogene homolog K (avian)	-1.09	2.72×10^{-1}	1.01	8.87×10^{-1}
BRAF	v-raf murine sarcoma viral oncogene homolog B1	-1.09	2.94×10^{-1}	-1.08	4.62×10^{-1}

PIM3	pim-3 oncogene	-1.09	1.28×10^{-1}	-1.02	6.60×10^{-1}
WNT7A	Wingless-type MMTV integration site family, member 7A	-1.10	1.56×10^{-1}	-1.01	7.82×10^{-1}
REL	v-rel reticuloendotheliosis viral oncogene homolog (avian)	-1.10	3.90×10^{-1}	-1.01	9.05×10^{-1}
CDON	Cdon homolog (mouse)	-1.10	9.39×10^{-2}	-1.10	1.27×10^{-1}
RAB20	RAB20, member RAS oncogene family	-1.10	1.83×10^{-1}	1.03	5.64×10^{-1}
MRAS	Muscle RAS oncogene homolog	-1.11	3.69×10^{-1}	-1.03	5.95×10^{-1}
CSF1R	Colony stimulating factor 1 receptor	-1.11	9.25×10^{-2}	1.02	6.44×10^{-1}
RAF1	v-raf-1 murine leukemia viral oncogene homolog 1	-1.11	1.74×10^{-1}	-1.21	8.95×10^{-3}
ADRB1	Adrenergic, beta-1-, receptor	-1.11	9.67×10^{-2}	1.08	2.08×10^{-1}
SKI	v-ski sarcoma viral oncogene homolog (avian)	-1.11	3.55×10^{-2}	1.08	7.68×10^{-2}
THRB	Thyroid hormone receptor, beta (erythroblastic leukemia viral (v-erb-a) oncogene homolog 2, avian)	-1.12	4.74×10^{-2}	-1.12	3.33×10^{-2}
FRAT1	Frequently rearranged in advanced T-cell lymphomas	-1.12	5.73×10^{-2}	1.01	8.37×10^{-1}
VAV1	vav 1 guanine nucleotide exchange factor	-1.13	3.25×10^{-2}	-1.00	9.95×10^{-1}
RAP1B	RAP1B, member of RAS oncogene family	-1.14	4.41×10^{-1}	-1.73	5.82×10^{-3}
RAB37	RAB37, member RAS oncogene family	-1.14	1.23×10^{-2}	1.08	2.00×10^{-1}
EEF1A1	Eukaryotic translation elongation factor 1 alpha 1	-1.14	2.38×10^{-1}	-1.16	8.13×10^{-2}
RAB42	RAB42, member RAS oncogene family	-1.14	1.74×10^{-1}	-1.01	8.90×10^{-1}
ABL1	c-abl oncogene 1, receptor tyrosine kinase	-1.14	1.85×10^{-2}	-1.08	2.07×10^{-1}
RABL2B	RAB, member of RAS oncogene family-like 2B	-1.15	1.66×10^{-2}	-1.20	4.97×10^{-3}

MAS1	MAS1 oncogene	-1.15	3.62×10^{-2}	1.02	8.03×10^{-1}
FES	Feline sarcoma oncogene	-1.16	6.14×10^{-3}	-1.05	2.91×10^{-1}
EVI1	Ecotropic viral integration site 1	-1.16	6.96×10^{-2}	-1.00	9.99×10^{-1}
RAPGEF1	Rap guanine nucleotide exchange factor (GEF) 1	-1.17	3.54×10^{-2}	-1.15	2.36×10^{-2}
PEA15	Phosphoprotein enriched in astrocytes 15	-1.18	1.23×10^{-1}	-1.26	5.63×10^{-2}
CXCL1	Chemokine (C-X-C motif) ligand 1 (melanoma growth stimulating activity, alpha)	-1.18	2.07×10^{-1}	1.14	2.77×10^{-1}
RAB40A	RAB40A, member RAS oncogene family	-1.19	2.68×10^{-3}	-1.05	3.04×10^{-1}
RAB31	RAB31, member RAS oncogene family	-1.20	1.56×10^{-1}	-1.09	4.61×10^{-1}
PDGFB	Platelet-derived growth factor beta polypeptide (simian sarcoma viral (v-sis) oncogene homolog)	-1.20	2.55×10^{-3}	-1.06	3.65×10^{-1}
RAP1A	RAP1A, member of RAS oncogene family	-1.21	6.05×10^{-2}	-1.27	1.90×10^{-2}
ERBB4	v-erb-a erythroblastic leukemia viral oncogene homolog 4 (avian)	-1.21	1.81×10^{-3}	-1.01	9.02×10^{-1}
USP6	Ubiquitin specific peptidase 6 (Tre-2 oncogene)	-1.22	9.09×10^{-3}	-1.10	1.22×10^{-1}
RABL2A	RAB, member of RAS oncogene family-like 2A	-1.22	7.63×10^{-3}	-1.24	7.50×10^{-3}
RRAS	Related RAS viral (r-ras) oncogene homolog	-1.23	3.91×10^{-3}	-1.09	1.81×10^{-1}
VAV3	vav 3 guanine nucleotide exchange factor	-1.23	1.18×10^{-2}	-1.27	7.05×10^{-3}
SPAG9	Sperm associated antigen 9	-1.24	5.45×10^{-2}	-1.31	5.09×10^{-2}
RHOA	ras homolog gene family, member A	-1.24	3.95×10^{-3}	-1.29	4.22×10^{-3}
RASEF	RAS and EF-hand domain containing	-1.25	3.74×10^{-3}	1.07	4.46×10^{-1}
THRA	Thyroid hormone receptor, alpha (erythroblastic leukemia viral (v-erb-a) oncogene homolog, avian)	-1.26	6.05×10^{-3}	-1.19	2.69×10^{-2}

MYBL1	v-myb myeloblastosis viral oncogene homolog (avian)-like 1	-1.26	1.63×10^{-2}	-1.09	2.27×10^{-1}
AXL	AXL receptor tyrosine kinase	-1.26	7.17×10^{-6}	-1.12	2.65×10^{-2}
RBM6	RNA binding motif protein 6	-1.27	4.86×10^{-2}	-1.29	7.04×10^{-2}
USP4	Ubiquitin specific peptidase 4 (proto-oncogene)	-1.28	2.69×10^{-3}	-1.39	9.25×10^{-4}
RAB17	RAB17, member RAS oncogene family	-1.30	1.70×10^{-4}	1.02	6.96×10^{-1}
FGR	Gardner-Rasheed feline sarcoma viral (v-fgr) oncogene homolog	-1.31	1.67×10^{-4}	-1.08	8.29×10^{-2}
CXCL3	Chemokine (C-X-C motif) ligand 3	-1.32	7.93×10^{-4}	1.11	8.52×10^{-2}
LYN	v-yes-1 Yamaguchi sarcoma viral related oncogene homolog	-1.34	1.16×10^{-2}	1.02	8.30×10^{-1}
NR2F1	Nuclear receptor subfamily 2, group F, member 1	-1.36	2.47×10^{-6}	-1.10	6.90×10^{-2}
MAP3K8	Mitogen-activated protein kinase kinase kinase 8	-1.36	7.46×10^{-5}	-1.22	9.21×10^{-3}
FYN	FYN oncogene related to SRC, FGR, YES	-1.38	6.05×10^{-4}	-1.62	3.58×10^{-5}
MAFF	v-maf musculoaponeurotic fibrosarcoma oncogene homolog F (avian)	-1.40	5.49×10^{-4}	-1.03	6.47×10^{-1}
RAB27A	RAB27A, member RAS oncogene family	-1.42	6.41×10^{-4}	-1.12	3.27×10^{-1}
ARHGEF12	Rho guanine nucleotide exchange factor (GEF) 12	-1.43	6.51×10^{-3}	-1.48	3.45×10^{-2}
JUND	jun D proto-oncogene	-1.44	1.75×10^{-8}	-1.13	5.28×10^{-3}
RHOB	ras homolog gene family, member B	-1.45	1.96×10^{-7}	-1.08	2.13×10^{-1}
ETS2	v-ets erythroblastosis virus E26 oncogene homolog 2 (avian)	-1.58	6.93×10^{-6}	-1.43	1.35×10^{-2}
JUNB	jun B proto-oncogene	-1.60	9.51×10^{-4}	-1.35	2.70×10^{-2}
FER	fer (fps/fes related) tyrosine kinase	-1.61	1.72×10^{-4}	-1.52	1.50×10^{-3}
ETS1	v-ets erythroblastosis virus E26	-1.67	1.63×10^{-4}	-1.63	1.55×10^{-4}

	oncogene homolog 1 (avian)				
FLI1	Friend leukemia virus integration 1	-1.68	1.69×10^{-8}	-1.63	7.05×10^{-6}
ERG	v-ets erythroblastosis virus E26 oncogene homolog (avian)	-1.72	4.38×10^{-8}	-1.36	2.34×10^{-3}
RAB8B	RAB8B, member RAS oncogene family	-1.76	1.24×10^{-3}	-1.92	3.62×10^{-4}
KIT	v-kit Hardy-Zuckerman 4 feline sarcoma viral oncogene homolog	-1.84	2.08×10^{-4}	-1.34	4.29×10^{-2}
AKAP13	A kinase (PRKA) anchor protein 13	-1.87	3.77×10^{-10}	-1.57	1.75×10^{-4}
AKT3	v-akt murine thymoma viral oncogene homolog 3 (protein kinase B, gamma)	-1.88	4.68×10^{-4}	-1.83	2.81×10^{-4}
KLF6	Kruppel-like factor 6	-1.97	6.09×10^{-9}	-1.46	2.99×10^{-4}
JUN	jun oncogene	-2.30	7.39×10^{-9}	-1.72	1.19×10^{-4}
FOS	v-fos FBJ murine osteosarcoma viral oncogene homolog	-2.80	7.18×10^{-7}	-2.02	9.18×10^{-4}
ROS1	c-ros oncogene 1 , receptor tyrosine kinase	-2.97	8.79×10^{-9}	-1.22	3.44×10^{-1}
CXCL2	Chemokine (C-X-C motif) ligand 2	-3.65	2.45×10^{-8}	-1.69	4.68×10^{-4}
FOSB	FBJ murine osteosarcoma viral oncogene homolog B	-4.65	1.60×10^{-9}	-2.14	4.87×10^{-4}

Table S5. Differential changes in tumor suppressors

Name	Description	SCC		ADC	
		fold-change	p-value	fold-change	p-value
DLG1	Discs, large homolog 1 (*Drosophila*)	2.41	3.46×10^{-5}	-1.15	3.72×10^{-1}
DLGAP5	Discs, large (*Drosophila*) homolog-associated protein 5	2.35	4.22×10^{-7}	1.42	1.13×10^{-4}
FAT	FAT tumor suppressor homolog 1 (*Drosophila*)	1.95	1.64×10^{-5}	1.34	2.29×10^{-2}
TRIM59	Tripartite motif-containing 59	1.55	8.23×10^{-5}	1.21	4.97×10^{-6}
FAT2	FAT tumor suppressor homolog 2 (*Drosophila*)	1.52	3.83×10^{-5}	1.10	6.39×10^{-2}
SMARCB1	SWI/SNF related, matrix associated, actin dependent regulator of chromatin, subfamily b, member 1	1.48	3.47×10^{-5}	1.10	1.62×10^{-1}
CDKN2A	Cyclin-dependent kinase inhibitor 2A (melanoma, p16, inhibits CDK4)	1.32	2.06×10^{-2}	1.26	1.15×10^{-3}
TUSC3	Tumor suppressor candidate 3	1.29	4.14×10^{-2}	-1.01	9.36×10^{-1}
ING2	Inhibitor of growth family, member 2	1.25	7.19×10^{-2}	1.18	2.65×10^{-1}
ST13	Suppression of tumorigenicity 13 (colon carcinoma) (Hsp70 interacting protein)	1.25	7.53×10^{-2}	-1.10	4.53×10^{-1}
EXT1	Exostoses (multiple) 1	1.19	1.50×10^{-1}	-1.07	3.64×10^{-1}
TP53	Tumor protein p53	1.18	6.27×10^{-2}	1.09	1.88×10^{-1}
VHL	von Hippel-Lindau tumor suppressor	1.17	1.60×10^{-2}	1.20	1.02×10^{-3}
BRCA2	Breast cancer 2, early onset	1.17	1.61×10^{-2}	1.02	6.07×10^{-1}
RB1	Retinoblastoma 1	1.15	1.57×10^{-1}	-1.40	1.93×10^{-3}
LATS1	LATS, large tumor suppressor, homolog 1 (*Drosophila*)	1.15	3.78×10^{-2}	-1.15	2.59×10^{-2}
POU6F2	POU class 6 homeobox 2	1.14	3.07×10^{-2}	1.10	1.35×10^{-1}

CELSR2	Cadherin, EGF LAG seven-pass G-type receptor 2 (flamingo homolog, *Drosophila*)	1.12	9.52×10^{-3}	1.10	4.80×10^{-3}
PDGFRL	Platelet-derived growth factor receptor-like	1.12	1.91×10^{-1}	1.15	1.60×10^{-2}
BAX	BCL2-associated X protein	1.10	5.67×10^{-2}	1.21	4.78×10^{-4}
EXT2	Exostoses (multiple) 2	1.09	1.17×10^{-1}	1.00	9.21×10^{-1}
RARB	Retinoic acid receptor, beta	1.09	2.37×10^{-1}	-1.12	9.82×10^{-2}
ING1	Inhibitor of growth family, member 1	1.08	1.68×10^{-1}	1.10	2.26×10^{-2}
FH	Fumarate hydratase	1.07	3.18×10^{-1}	1.06	4.42×10^{-1}
EAF2	ELL associated factor 2	1.07	3.09×10^{-1}	1.06	2.95×10^{-1}
ING4	Inhibitor of growth family, member 4	1.07	2.85×10^{-1}	-1.01	8.93×10^{-1}
FAM123B	Family with sequence similarity 123B	1.06	2.78×10^{-1}	1.06	2.86×10^{-1}
ST7L	Suppression of tumorigenicity 7 like	1.05	2.52×10^{-1}	-1.04	2.28×10^{-1}
STEAP3	STEAP family member 3	1.05	2.84×10^{-1}	1.15	3.35×10^{-3}
SMAD2	SMAD family member 2	1.04	7.32×10^{-1}	1.04	7.07×10^{-1}
FAM10A4	Family with sequence similarity 10, member A4 pseudogene	1.04	5.94×10^{-1}	1.00	9.97×10^{-1}
CEBPA	CCAAT/enhancer binding protein (C/EBP), alpha	1.02	6.95×10^{-1}	1.30	3.27×10^{-5}
MN1	Meningioma (disrupted in balanced translocation) 1	1.02	7.36×10^{-1}	1.16	7.45×10^{-3}
PTCH1	Patched homolog 1 (*Drosophila*)	1.01	8.18×10^{-1}	-1.04	3.97×10^{-1}
Pinx1	PIN2-interacting protein 1	1.01	9.32×10^{-1}	1.09	1.86×10^{-1}
TUSC2	Tumor suppressor candidate 2	1.00	9.53×10^{-1}	1.15	4.09×10^{-3}
DLEU1	Deleted in lymphocytic leukemia 1 (non-protein coding)	-1.00	1.00	-1.01	9.22×10^{-1}
LZTS2	Leucine zipper, putative tumor suppressor 2	-1.00	9.07×10^{-1}	1.02	6.23×10^{-1}

GLTSCR1	Glioma tumor suppressor candidate region gene 1	-1.00	9.22×10^{-1}	1.11	4.39×10^{-2}
CDKN1B	Cyclin-dependent kinase inhibitor 1B (p27, Kip1)	-1.01	9.27×10^{-1}	-1.09	3.39×10^{-1}
CDKN2B	Cyclin-dependent kinase inhibitor 2B (p15, inhibits CDK4)	-1.01	8.38×10^{-1}	1.20	3.78×10^{-3}
TUSC4	Tumor suppressor candidate 4	-1.02	6.06×10^{-1}	1.09	3.35×10^{-2}
OVCA2	Candidate tumor suppressor in ovarian cancer 2	-1.03	4.47×10^{-1}	1.06	7.07×10^{-2}
ARL11	ADP-ribosylation factor-like 11	-1.03	5.57×10^{-1}	-1.02	7.04×10^{-1}
TUSC1	Tumor suppressor candidate 1	-1.04	4.24×10^{-1}	1.10	2.77×10^{-2}
RPH3AL	Rabphilin 3A-like (without C2 domains)	-1.05	2.56×10^{-1}	1.23	1.24×10^{-4}
RASSF5	Ras association (RalGDS/AF-6) domain family member 5	-1.05	3.58×10^{-1}	-1.04	5.09×10^{-1}
SMAD4	SMAD family member 4	-1.05	5.53×10^{-1}	-1.25	3.24×10^{-2}
TUSC5	Tumor suppressor candidate 5	-1.06	4.42×10^{-1}	1.06	3.31×10^{-1}
CDK2AP2	Cyclin-dependent kinase 2 associated protein 2	-1.08	2.48×10^{-1}	1.21	4.60×10^{-4}
RASSF4	Ras association (RalGDS/AF-6) domain family member 4	-1.09	3.73×10^{-1}	1.07	1.88×10^{-1}
NKX3-1	NK3 homeobox 1	-1.09	1.07×10^{-1}	1.04	4.59×10^{-1}
LZTS1	Leucine zipper, putative tumor suppressor 1	-1.09	1.90×10^{-1}	1.08	1.94×10^{-1}
APC	Adenomatous polyposis coli	-1.09	3.95×10^{-1}	-1.29	9.09×10^{-4}
PTEN	Phosphatase and tensin homolog	-1.09	3.01×10^{-1}	-1.03	6.85×10^{-1}
CYB561D2	Cytochrome b-561 domain containing 2	-1.10	1.39×10^{-1}	1.04	5.50×10^{-1}
VHLL	von Hippel-Lindau tumor suppressor-like	-1.13	5.81×10^{-2}	-1.04	5.23×10^{-1}
FLCN	Folliculin	-1.13	2.29×10^{-2}	1.04	3.91×10^{-1}
RASSF1	Ras association (RalGDS/AF-6) domain family member 1	-1.15	4.18×10^{-2}	1.06	1.81×10^{-1}

LATS2	LATS, large tumor suppressor, homolog 2 (*Drosophila*)	-1.15	2.82×10^{-3}	1.02	5.47×10^{-1}
RPL10	Ribosomal protein L10	-1.17	1.78×10^{-1}	1.05	7.52×10^{-1}
GLTSCR2	Glioma tumor suppressor candidate region gene 2	-1.18	2.94×10^{-3}	-1.13	6.14×10^{-2}
SPI1	Spleen focus forming virus (SFFV) proviral integration oncogene spi1	-1.20	4.56×10^{-3}	1.05	2.56×10^{-1}
HYAL1	Hyaluronoglucosaminidase 1	-1.20	5.25×10^{-4}	-1.10	4.64×10^{-2}
FAT3	FAT tumor suppressor homolog 3 (*Drosophila*)	-1.20	5.88×10^{-4}	-1.07	2.91×10^{-1}
MTUS1	Mitochondrial tumor suppressor 1	-1.25	4.10×10^{-2}	-1.08	5.09×10^{-1}
DCC	Deleted in colorectal carcinoma	-1.27	1.47×10^{-3}	-1.14	4.26×10^{-2}
FAT4	FAT tumor suppressor homolog 4 (*Drosophila*)	-1.44	1.87×10^{-7}	-1.43	3.55×10^{-7}
CADM1	Cell adhesion molecule 1	-1.98	1.00×10^{-7}	-1.24	3.08×10^{-2}
TGFBR2	Transforming growth factor, beta receptor II (70/80 kDa)	-2.09	1.85×10^{-11}	-1.81	2.09×10^{-7}